0090-9556/09/3702-272–276$20.00
DRUG METABOLISM AND DISPOSITION
Vol. 37, No. 2
24208/3426314
Printed in U.S.A.
Copyright © 2009 by The American Society for Pharmacology and Experimental Therapeutics
DMD 37:272–276, 2009

Short Communication

Close Association of *UGT1A9* IVS1+399C>T with *UGT1A1*28*, **6*, or **60* Haplotype and Its Apparent Influence on 7-Ethyl-10-hydroxycamptothecin (SN-38) Glucuronidation in Japanese

Received August 26, 2008; accepted October 30, 2008

ABSTRACT:

The anticancer prodrug, irinotecan, is converted to its active form 7-ethyl-10-hydroxycamptothecin (SN-38) by carboxylesterases, and SN-38 is inactivated by UDP-glucuronosyltransferase (UGT)1A1-mediated glucuronidation. UGT1A9 also mediates this reaction. In a recent study, it was reported that the *UGT1A9* IVS1+399 (I399)C>T polymorphism is associated with increased SN-38 glucuronidation both in vitro and in vivo. However, its role in UGT1A9 expression levels and activity is controversial. Thus, we evaluated the role of I399C>T in SN-38 glucuronidation using 177 Japanese cancer patients administered irinotecan. I399C>T was detected at a 0.636 allele frequency. This polymorphism was in strong linkage disequilibrium (LD) with *UGT1A9*1b* (−126_−118T_9>T_{10}, |D′| = 0.99) and *UGT1A1*6* (211G>A, 0.86), in moderate LD with *UGT1A1*60* (−3279T>G, 0.55), but weakly associated with *UGT1A1*28* (−54_−39A(TA)$_6$TAA>A(TA)$_7$TAA, 0.25). Haplotype analysis showed that 98% of the I399C alleles were linked with low-activity haplotypes, either *UGT1A1*6*, **28*, or **60*. On the other hand, 85% of the T alleles were linked with the *UGT1A1* wild-type haplotype **1*. Although I399T-dependent increases in SN-38 glucuronide/SN-38 area under concentration-time curve (AUC) ratio (an in vivo marker for UGT1A activity) and decreases in SN-38 AUC/dose were apparent ($P < 0.0001$), these effects were no longer observed after stratified patients by *UGT1A1*6*, **28*, or **60* haplotype. Thus, at least in Japanese populations, influence of I399C>T on SN-38 glucuronidation is attributable to its close association with either *UGT1A1*6*, **28*, or **60*.

Irinotecan is an important drug for treatment of various tumors including lung, colon, and gastric (Smith et al., 2006). The infused drug is metabolized to its active form 7-ethyl-10-hydroxycamptothecin (SN-38) by carboxylesterases, and SN-38 is inactivated by glucuronidation. At least four UDP-glucuronosyltransferase (UGT) isoforms, namely UGT1A1, UGT1A7, UGT1A9, and UGT1A10, are known to glucuronidate SN-38 (Gagné et al., 2002; Saito et al., 2007).

The UGT1A gene complex consists of 9 active first exons including *UGT1A10*, *1A9*, *1A7*, and *1A1* (in this order) and common exons 2 to 5. One of the 9 first exons can be used in conjunction with the common exons (Tukey and Strassburg, 2000). The UGT1A N-terminal domains (encoded by the first exons) determine substrate-binding specificity, and the C-terminal domain (encoded by exons 2 to 5) is important for binding to UDP-glucuronic acid. The 5′- or 3′-flanking region of each exon 1 is presumably involved in regulation of its expression. Substantial interindividual differences have been detected in mRNA and protein levels and enzymatic activity of the UGT1A isoforms (Fisher et al., 2000; Saito et al., 2007).

SN-38 glucuronidation is thought to be mediated mainly by UGT1A1, and its genetic polymorphisms affecting irinotecan pharmacokinetics and adverse reactions have been already identified. The TA-repeat polymorphism, −54_−39A(TA)$_6$TAA>A(TA)$_7$TAA (*UGT1A1*28* allele), is associated with lower promoter activity, resulting in reduced SN-38 glucuronidation (Beutler et al., 1998; Iyer et al., 1999). The single nucleotide polymorphism (SNP) 211G>A (Gly71Arg, **6* allele), found mainly in East Asians, causes reduced protein expression levels and SN-38 glucuronidation activity (Gagné et al., 2002; Jinno et al., 2003). Another SNP in the enhancer region of *UGT1A1*, −3279T>G (**60* allele), is also a causative factor for reduced expression (Sugatani et al., 2002). Allele frequencies have been reported for **28* (0.09–0.13), **6* (0.15–0.19), and **60* (0.26–0.32) in Japanese and Chinese populations and for **28* (0.30–0.39), **6* (~0), and **60* (0.44–0.55) in whites (Saito et al., 2007). In a previous study, in the Japanese population, we defined haplotype **28* as the haplotype harboring the **28* allele, haplotype **6* as that harboring the**6* allele, and haplotype **60* as that harboring the **60* allele (and without the **28* or **6* allele) (Sai et al., 2004; Saeki et al., 2006). Note that most of the **28* haplotypes concurrently harbored the **60* alleles, and that the **28* and **6* alleles were exclusively present on the different chromosomes (Sai et al., 2004; Saeki et al., 2006). We have also revealed that the haplotype **28*, **6*, or **60* was associated with reduced SN-38 glucuronide (SN-38G)/SN-38 area under concentration-time curve (AUC) ratios, an in vivo parameter for UGT1A activity (Minami et al., 2007).

In a recent study, an intronic SNP of *UGT1A9*, IVS1+399 (I399)C>T, has been shown to be associated with increased UGT1A9 protein levels and glucuronidation activities toward SN-38 and the UGT1A9 probe drug propofol (Girard et al., 2006). Elevation of

This study was supported in part by the program for the Promotion of Fundamental Studies in Health Sciences from the National Institute of Biomedical Innovation [Grant 05-25]; and a Health and Labour Sciences Research grant from the Ministry of Health, Labour and Welfare in Japan [Grant KHB1008].

Y.S. and K.S. contributed equally to this work.

Article, publication date, and citation information can be found at http://dmd.aspetjournals.org.

doi:10.1124/dmd.108.024208.

ABBREVIATIONS: SN-38, 7-ethyl-10-hydroxycamptothecin; UGT, UDP-glucuronosyltransferase; SNP, single nucleotide polymorphism; SN-38G, SN-38 glucuronide; AUC, area under concentration-time curve; I399, *UGT1A9* IVS1+399; LD, linkage disequilibrium.

SN-38 glucuronidation activity by this SNP is significant among subjects without *UGT1A1*28*. Sandanaraj et al. (2008) have also reported that I399C/C patients showed higher SN-38 AUC than C/T and T/T patients. With the same *UGT1A1* diplotypes, patients with I399T/T (and *UGT1A9* $-126\_-118T_{10}/T_{10}$) have shown higher SN-38G C_{max} than I399C/T (and T_9/T_{10}) patients. *UGT1A9*1b* (*UGT1A9* $-126\_-118T_9>T_{10}$) has been shown to have no affect on UGT1A9 expression levels (Girard et al., 2006; Ramírez et al., 2007; Sandanaraj et al., 2008). Thus, two groups did suggest that I399T allele was associated with higher glucuronidation activity. However, using human liver microsomes, Ramírez et al. (2007) showed that I399C>T had no significant effect on both UGT1A9 mRNA levels and glucuronidation activities for two UGT1A9 substrates. Therefore, the roles of I399C>T in UGT1A9 activities as well as SN-38 glucuronidation remain inconclusive.

In the present report, we reveal the linkage of I399C>T with *UGT1A1*, *UGT1A7*, and *UGT1A9* polymorphisms and analyze its association with the SN-38G/SN-38 AUC ratio and SN-38 AUC/dose (per dose) to clarify its role in SN-38 glucuronidation.

Materials and Methods

Patients. One hundred and seventy-seven patients (81 lung, 63 colon, 19 stomach, and 14 other cancer patients) administered irinotecan at the National Cancer Center were enrolled in this study as described previously (Minami et al., 2007). This study was approved by the ethics committees of the National Cancer Center and the National Institute of Health Sciences, and written informed consent was obtained from all participants. Eligibility criteria, patient profiles, and irinotecan regimens are summarized in our previous report (Minami et al., 2007). In brief, patients consisted of 135 males and 42 females with a mean age of 60.5 (26–78 years old), and their performance status was 0 (84 patients), 1 (89 patients), or 2 (4 patients). Irinotecan administrations were conducted according to the standard protocols in Japan as follows: i.v. 90-min infusion at a dose of 100 mg/m^2 weekly or 150 mg/m^2 biweekly in irinotecan monotherapy; and 60 mg/m^2 weekly with cisplatin in most combination therapies.

Genotyping and Haplotype Analysis. Genomic DNA was extracted from whole blood of 177 irinotecan-administered patients (Saeki et al., 2006). *UGT1A9* IVS1+399C>T (rs2741049) was genotyped using the TaqMan SNP Genotyping Assay kit (C_9096281_10) according to the manufacturer's instructions (Applied Biosystems, Foster City, CA). The *UGT1A1*28* allele [$-54\_-39A(TA)_6TAA>A(TA)_7TAA$], *UGT1A1*6* allele [211G>A (Gly71Arg)], *UGT1A1*60* allele (−3279T>G), *UGT1A7*2* haplotype [387T>G, 391C>A and 392G>A (Asn129Lys and Arg131Lys)], *UGT1A7*3* haplotype [387T>G, 391C>A, 392G>A, and 622T>C (Asn129Lys, Arg131Lys, and Trp208Arg)], and *UGT1A9*1b* allele ($-126\_-118T_9>T_{10}$) were determined previously (Saeki et al., 2006). Hardy-Weinberg equilibrium analysis of I399C>T, linkage disequilibrium (LD) analysis of the *UGT1A9*, *UGT1A7*, and *UGT1A1* polymorphisms, and haplotype estimation with an expectation-maximization algorithm were performed using SNPAlyze version 7.0 software (Dynacom, Chiba, Japan).

Pharmacokinetics. Pharmacokinetic data for the 176 irinotecan-treated patients (data for one patient was unavailable) were described previously (Minami et al., 2007). In brief, heparinized blood was collected before irinotecan administration and at 0, 0.33, 1, 2, 4, 8, and 24 h after termination of the first infusion of irinotecan. SN-38 and SN-38G plasma concentrations were determined by high-performance liquid chromatography, and AUC was calculated using the trapezoidal method in WinNonlin version 4.01 (Pharsight, Mountain View, CA).

Statistical Analysis. Gene dose effects of I399C>T and *UGT1A1* haplotypes (**28*, **6*, *or *60*) were assessed by the Jonckheere-Terpstra test using StatExact version 6.0 (Cytel Inc., Cambridge, MA). Multiplicity adjustment was conducted with the false discovery rate. The significant difference was set at $p = 0.05$ (two-tailed).

Results

Linkages of *UGT1A9* IVS1+399 (I399)C>T with Other Polymorphisms. In our patients, I399C>T was detected at a 0.636 allele frequency, which is almost the same as those in the HapMap data (rs2741049) for Japanese (0.663) and Han Chinese (0.633) populations, but higher than those for Europeans (0.383) and Sub-Saharan Africans (Yoruba) (0.417). Genotype distribution for this SNP was in Hardy-Weinberg equilibrium ($p = 0.418$). LD analysis was performed between I399C>T and the previously determined genotypes, *UGT1A9*1b*, *UGT1A7*2* and **3*, and *UGT1A1*28*, **6*, and **60*, which were detected at >0.1 frequencies in Japanese populations (Saeki et al., 2006). When assessed by the |D'| value, I399C>T was in complete LD with *UGT1A7* 387T>G, 391C>A and 392G>A (*UGT1A7*2*, |D'| = 1.000); in strong LD with *UGT1A9* $-126\_-118T_9>T_{10}$ (*UGT1A9*1b*, 0.987), *UGT1A7* 622T>C (*UGT1A7*3*, 0.977), and *UGT1A1* 211G>A (*UGT1A1*6*, 0.864); and in moderate LD with *UGT1A1* −3279T>G (*UGT1A1*60*, 0.554), but weakly associated with *UGT1A1* $-54\_-39A(TA)_6TAA>A(TA)_7TAA$ (*UGT1A1*28*, 0.252). In r^2 values, the I399C>T was in strong LD with *UGT1A7*2* ($r^2 = 0.976$) and *UGT1A9*1b* (0.916), in moderate LD with *UGT1A7*3* (0.478), but in weak LD with *UGT1A1*6* (0.261) and *UGT1A1*60* (0.208), and in little LD with *UGT1A1*28* (0.018).

Haplotype Analysis. Haplotype analysis was performed using the 9 polymorphisms including I399C>T. As shown in Fig. 1, 95% (123/129) of the I399C alleles were linked with the *UGT1A9* -126_-118T_9 alleles, and 100% (225/225) of the T alleles were linked with the T_{10} alleles (*UGT1A9*1b*). The I399C alleles were completely (129/129) linked with the *UGT1A7* 387G, 391A, and 392A alleles, and most T alleles (223/225) were linked with the 387T, 391C, and 392G alleles. The 40% (51/129) and 60% (78/129) of the I399C alleles were linked with *UGT1A7*2* and *UGT1A7*3* haplotypes, respectively. We also found that 98% (126/129) of the I399C alleles were linked with the *UGT1A1*6* (211G>A), **28* [$-54\_-39A(TA)_6TAA>A(TA)_7TAA$], or **60* (−3279T>G). According to the *UGT1A1* haplotype definition by Sai et al. (2004), 42% (54/129), 36% (46/129), 19% (25/129), and 1% (1/129) of the I399C alleles were linked with the *UGT1A1* haplotypes **6a* (harboring **6* allele), **60a* (harboring **60* allele), **28b* (harboring **60* and**28* alleles), and **28d* (harboring **28* allele), respectively. On the other hand, 85% (191/225) of the T alleles were linked with the *UGT1A1* wild-type haplotype **1*.

Association Analysis. The associations of I399C>T with irinotecan pharmacokinetic parameters were then analyzed using the estimated haplotypes. First, association with SN-38G/SN-38 AUC ratio, an in vivo parameter of UGT1A activity (Sai et al., 2004; Minami et al., 2007; Sandanaraj et al., 2008), was analyzed. *UGT1A7*2* had unchanged activity for SN-38 glucuronidation (Gagné et al., 2002), and neither *UGT1A9*1b* nor *UGT1A7*3* had significant effects on the SN-38G/SN-38 AUC ratio in our previous study (Minami et al., 2007). On the other hand, the *UGT1A1*6*, **28*, and **60* haplotypes were associated with the reduced SN-38G/SN-38 AUC ratios (Minami et al., 2007). Although effects of the haplotype **28* and **6* were more striking, haplotype *UGT1A1*60*, harboring only the **60* allele without the **28* allele, was weakly associated with the reduced ratio. To remove even this weak effect and clarify the real effect of I399C>T, *UGT1A1*60* was also considered as low-activity haplotype in this analysis. Namely, we analyzed the associations of I399C>T with the AUC ratio within the groups stratified by the *UGT1A1* haplotypes, *UGT1A1*28* (**28b* and **28d*), **6* (**6a*), and **60* (**60a*) (combined and shown as *UGT1A1*"+").

When stratified by the I399C>T genotype, a T allele-dependent

Gene		*UGT1A9*		*UGT1A7*[2]				*UGT1A1*[3]			Number	Frequency
Nucleotide change		-126_-118 T_9>T_{10}	IVS1+399 C>T	387 T>G	391 C>A	392 G>A	622 T>C	-3279 T>G	$(TA)_6$>$(TA)_7$	211 G>A		
Allele name		*1b		*2, *3	*2, *3	*2, *3	*3	*60, *28	*28	*6		
Haplotypes[1]	*1C-*3-*6a			■	■	■	■			■	47	0.133
	*1C-*2-*60a			■	■	■		■			44	0.124
	*1C-*3-*28b			■	■	■	■	■	■		21	0.059
	*1C-*2-*28b			■	■	■		■	■		4	0.011
	*1C-*3-*60a			■	■	■	■	■			2	0.006
	*1C-*3-*28d			■	■	■	■		■		1	0.003
	*1C-*2-*6a			■	■	■				■	1	0.003
	*1bC-*3-*6a	■		■	■	■	■			■	6	0.017
	*1C-*2-*1			■	■	■					2	0.006
	*1C-*3-*1			■	■	■	■				1	0.003
	*1bT-*1-*1	■	■								190	0.537
	*1bT-*3-*1	■	■	■	■	■	■				1	0.003
	*1bT-*1-*28b	■	■					■	■		22	0.062
	*1bT-*1-*60a	■	■					■			5	0.014
	*1bT-*1-*6a	■	■							■	5	0.014
	*1bT-*1-*28d	■	■						■		1	0.003
	*1bT-*2-*60a	■	■	■	■	■		■			1	0.003
Alelle frequency		0.653	0.636	0.370	0.370	0.370	0.223	0.280	0.138	0.167	354	1.000

FIG. 1. Haplotypes assigned by using common *UGT1A9*, *UGT1A7*, and *UGT1A1* polymorphisms. [1]Haplotypes were shown as *UGT1A9* haplotypes − *UGT1A7* haplotypes − *UGT1A1* haplotypes. Major allele, white blocks; minor allele, gray blocks. **1C*, T_9 and I399C; **1bC*, T_{10} and I399C; **1bT*, T_{10} and I399T in *UGT1A9*. [2]*UGT1A7**2* and **3* are the haplotypes harboring the three and four *UGT1A7* alleles, respectively. [3]*UGT1A1* $(TA)_6$>$(TA)_7$ indicates −54_−39A$(TA)_6$TAA>A$(TA)_7$TAA.

increase in the SN-38G/SN-38 AUC ratio was observed ($p < 0.0001$, Jonckheere-Terpstra test) (Fig. 2A). However, this trend was obviously dependent on biased distributions of *UGT1A1* haplotypes; e.g., 96% of the I399C/C patients were homozygotes for *UGT1A1*28*, **6*, *or *60*; and "*UGT1A1*28*, **6*, or **60*"-dependent reduction of SN-38G/SN-38 AUC ratio was found within the I399T/T genotypes ($p < 0.05$). As shown in Fig. 2B, *UGT1A1*28*, **6*, or **60* (*UGT1A1+*)-dependent reduction in the SN-38G/SN-38 ratio was observed when patients were stratified by these three haplotypes. However, no significant effect of I399C>T was found within the stratified patients ($p > 0.05$ within the −/−, −/+, or +/+ patient group in Fig. 2B). As for SN-38 AUC/dose (SN-38 AUC values adjusted by the doses used), a similar *UGT1A1* haplotype dependence was observed. Although the I399T-dependent reduction of SN-38 AUC/dose was detected ($p < 0.0001$), biased distributions of the *UGT1A1*28*, **6*, or **60* were again evident, and the *UGT1A1* + haplotypes-dependent increase was significant within the I399 C/T and T/T patients ($p < 0.01$ and $p < 0.05$, respectively) (Fig. 2C). Moreover, no significant effect of I399C>T on SN-38 AUC/dose was found when stratified by the *UGT1A1* haplotypes ($p > 0.05$ within the −/−, −/+, or +/+ patient group in Fig. 2D).

Discussion

In the present study, LD between I399C>T and *UGT1A1*, *UGT1A7*, or *UGT1A9* polymorphisms in Japanese populations was shown for the first time. Moreover, the apparent effect of I399C>T on SN-38 glucuronidation in Japanese cancer patients was suggested to result from its close association with *UGT1A1*28*, **6*, or **60*.

As for the influence of I399C>T on UGT1A9 activity, conflicting results have been reported. Girard et al. (2006) have shown that I399C>T was associated with increased UGT1A9 protein levels and enzyme activity toward an UGT1A9 probe drug propofol using 48 human liver microsomes derived mainly from whites. In contrast, using human liver microsomes from 46 white subjects, Ramírez et al. (2007) have revealed that the I399C>T had no significant effects on UGT1A9 mRNA levels and in vitro glucuronidation activities toward the two UGT1A9 substrates, flavopiridol and mycophenolic acid. Furthermore, another report has demonstrated that I399C>T had no influence on the pharmacokinetic parameters (such as AUC and C_{max}) of mycophenolic acid in 80 Japanese renal transplant recipients (Inoue et al., 2007). Thus, these latter two studies did suggest that the I399C>T polymorphism has no effect on UGT1A9 enzymatic activity. Note that, at least for Japanese populations, no study has reported that I399C>T affects UGT1A9 activity.

As for the influence of I399C>T on SN-38 glucuronidation, a possible enhancing effect has been suggested. Girard et al. (2006) have shown an increasing effect of I399C>T on SN-38 glucuronidation, and that this SNP did not show any close linkages with the *UGT1A1*28* or **60* allele ($r^2 < 0.06$). In addition, Sandanaraj et al. (2008) have reported that in 45 Asians consisting of Chinese (80%), Malay (18%), and others (2%), I399C/C patients had higher SN-38 AUC than C/T and T/T patients. Again, this SNP was not in LD with the *UGT1A1*28*, **6*, or **60* allele (r^2 were <0.09). Furthermore, association of I399T with increased SN-38G C_{max} has been observed even after stratified patients by *UGT1A1* genotypes, although the study sample size was small. These findings suggest that the I399T

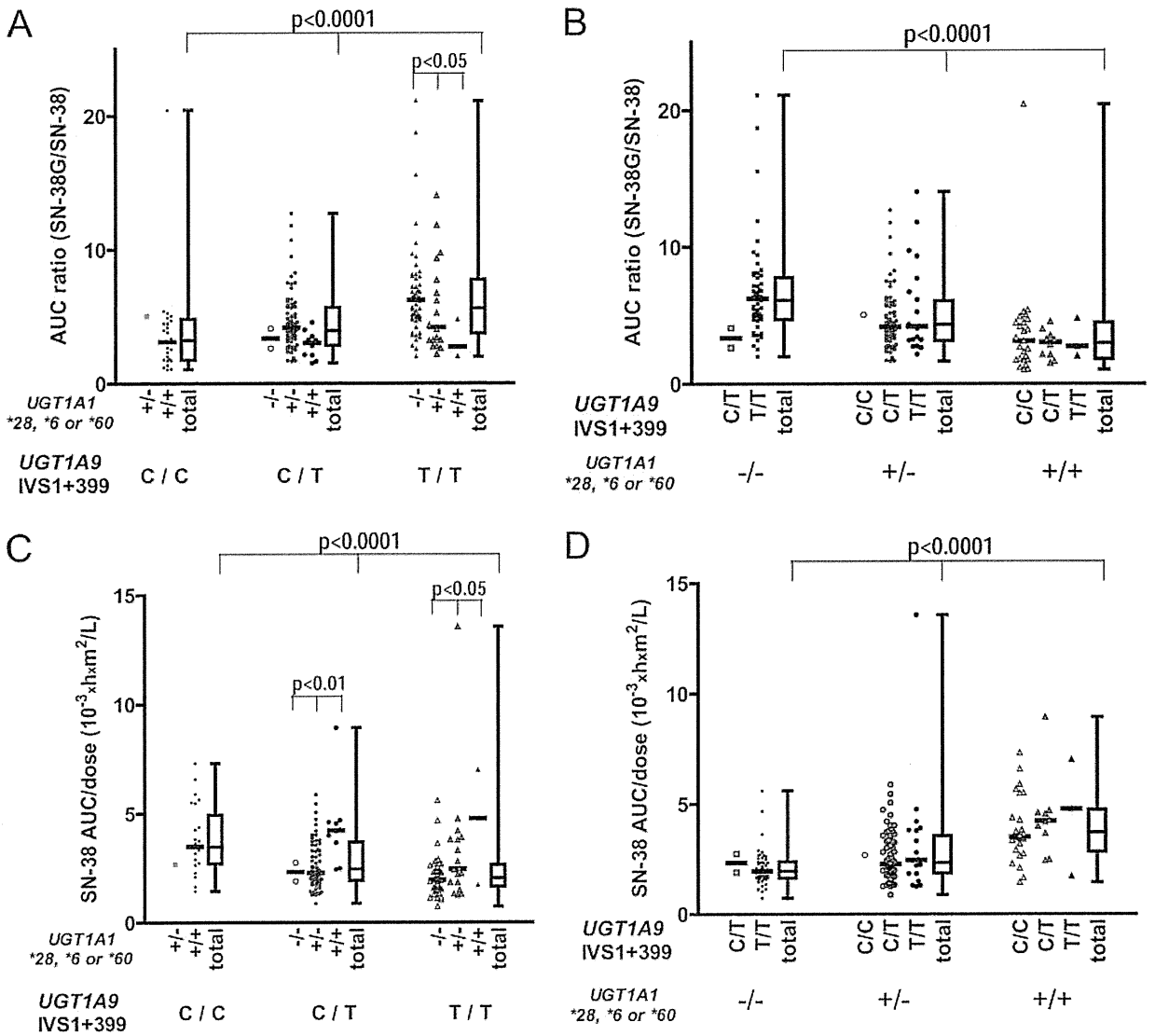

FIG. 2. Association analysis of *UGT1A9* IVS1+399 (I399)C>T with SN-38G/SN-38 AUC ratio (A and B) and SN-38 AUC/dose (C and D). A and C, I399 C/C, C/T, and T/T patients were further divided by the presence of *UGT1A1*28*, **6*, or **60* haplotypes: −/−, no *UGT1A1*28*, **6*, or **60*; −/+, heterozygotes for either *UGT1A1*28*, **6*, or **60*; +/+, homozygotes or compound heterozygotes for either *UGT1A1*28*, **6*, or **60*. B and D, *UGT1A1* −/−, −/+, and +/+ patients were further divided by I399 C/C, C/T, and T/T genotypes. Gene dose effects of I399C>T and the *UGT1A1* + haplotype were assessed by the Jonckheere-Terpstra test.

allele was associated with increased glucuronidation activity for SN-38 without linkages with the *UGT1A1* polymorphisms. Our data demonstrate that an increase in SN-38G/SN-38 AUC ratio (i.e., increased glucuronidation activity) was also found with I399C>T; however, after stratified patients by the *UGT1A1*6*, **28*, or **60* haplotypes (haplotype+) showing reduced SN-38 glucuronidation activity (Sai et al., 2004; Minami et al., 2007), any significant effect of the I399C>T was no longer observed. Thus, no direct effect of I399C>T on SN-38 glucuronidation was shown in the current study in Japanese populations. The discrepancy between our study and others might be derived from ethnic and/or population differences in haplotype distribution. In fact, in our Japanese population, 98% of the I399C alleles were linked with either *UGT1A1 *6*, **28*, or **60*, whereas 85% of the T alleles were linked with *UGT1A1*1*. On the other hand, in Sandanaraj's report (in Chinese + Malay), 84% of the I399C alleles were linked with *UGT1A1 *6*, **28*, or **60*, whereas only 67% of the T alleles were linked with *UGT1A1*1* (Sandanaraj et al., 2008).

In irinotecan therapies, genetic polymorphisms leading to increases in SN-38 AUC, which closely correlates with increased risk of severe neutropenia (Minami et al., 2007), are clinically important. The current study also demonstrated no significant influence of I399C>T on SN-38 AUC/dose after stratified patients by *UGT1A1* haplotypes. Consistent with this finding, no influence of this SNP was observed on the incidence of grade 3 or 4 neutropenia after irinotecan therapy in our population (data not shown). Recently, genetic testing of *UGT1A1*6* and **28*, which are related to severe neutropenia in Japanese populations, has been approved for clinical application in Japan. This study indicates that there is no clinical necessity for additional genotyping of I399C>T, at least in Japanese populations.

In conclusion of this study, the apparent influence of I399 (*UGT1A9* IVS1+399)C>T on SN-38 glucuronidation is attributable to its close association with *UGT1A1*6*, **28*, or **60* in the Japanese population. Furthermore, additional genotyping of I399C>T for personalized irinotecan therapy seems to be clinically irrelevant for Japanese populations.

Acknowledgments. We thank Chie Sudo for secretarial assistance.

Project Team for Pharmacogenetics (Y.S., K.Sa., K.M., N.K., J.S.), YOSHIRO SAITO
KIMIE SAI
Division of Functional Biochemistry and Genomics (Y.S., K.Sa., K.M., J.S.), KEIKO MAEKAWA
NAHOKO KANIWA
Division of Medicinal Safety Science (N.K.), KUNIAKI SHIRAO[1]
National Institute of Health Sciences, Tokyo, Japan; TETSUYA HAMAGUCHI
NOBORU YAMAMOTO
Gastrointestinal Oncology Division (K.Sh., T.H., Y.Y.), HIDEO KUNITOH
YUICHIRO OHE
Thoracic Oncology Division (N.Y., H.K., Y.O., T.T.), YASUHIDE YAMADA
TOMOHIDE TAMURA
National Cancer Center Hospital, Genetics Division (T.Y.), TERUHIKO YOSHIDA
HIRONOBU MINAMI[2]
National Cancer Center Research Institute, National Cancer Center, Tokyo, Japan; ATSUSHI OHTSU
YASUHIRO MATSUMURA
NAGAHIRO SAIJO
Division of Oncology/Hematology (H.M.), Division of Gastrointestinal Oncology/Digestive Endoscopy (A.O.), Investigative Treatment Division, Research Center for Innovative Oncology (Y.M.), Deputy Director (N.S.), National Cancer Center Hospital East, Kashiwa, Japan JUN-ICHI SAWADA

[1] Current affiliation: Department of Medical Oncology, Oita University Faculty of Medicine, Yufu, Japan.

[2] Current affiliation: Medical Oncology, Department of Medicine, Kobe University Hospital and Graduate School of Medicine, Kobe, Japan.

References

Beutler E, Gelbart T, and Demina A (1998) Racial variability in the UDP-glucuronosyltransferase 1 (UGT1A1) promoter: a balanced polymorphism for regulation of bilirubin metabolism? *Proc Natl Acad Sci U S A* **95:**8170–8174.

Fisher MB, Vandenbranden M, Findlay K, Burchell B, Thummel KE, Hall SD, and Wrighton SA (2000) Tissue distribution and interindividual variation in human UDP-glucuronosyltransferase activity: relationship between UGT1A1 promoter genotype and variability in a liver bank. *Pharmacogenetics* **10:**727–739.

Gagné JF, Montminy V, Belanger P, Journault K, Gaucher G, and Guillemette C (2002) Common human UGT1A polymorphisms and the altered metabolism of irinotecan active metabolite 7-ethyl-10-hydroxycamptothecin (SN-38). *Mol Pharmacol* **62:**608–617.

Girard H, Villeneuve L, Court MH, Fortier LC, Caron P, Hao Q, von Moltke LL, Greenblatt DJ, and Guillemette C (2006) The novel UGT1A9 intronic I399 polymorphism seems as a predictor of 7-ethyl-10-hydroxycamptothecin glucuronidation levels in the liver. *Drug Metab Dispos* **34:**1220–1228.

Inoue K, Miura M, Satoh S, Kagaya H, Saito M, Habuchi T, and Suzuki T (2007) Influence of UGT1A7 and UGT1A9 intronic I399 genetic polymorphisms on mycophenolic acid pharmacokinetics in Japanese renal transplant recipients. *Ther Drug Monit* **29:**299–304.

Iyer L, Hall D, Das S, Mortell MA, Ramírez J, Kim S, Di Rienzo A, and Ratain MJ (1999) Phenotype-genotype correlation of in vitro SN-38 (active metabolite of irinotecan) and bilirubin glucuronidation in human liver tissue with UGT1A1 promoter polymorphism. *Clin Pharmacol Ther* **65:**576–582.

Jinno H, Tanaka-Kagawa T, Hanioka N, Saeki M, Ishida S, Nishimura T, Ando M, Saito Y, Ozawa S, and Sawada J (2003) Glucuronidation of 7-ethyl-10-hydroxycamptothecin (SN-38), an active metabolite of irinotecan (CPT-11), by human UGT1A1 variants, G71R, P229Q, and Y486D. *Drug Metab Dispos* **31:**108–113.

Minami H, Sai K, Saeki M, Saito Y, Ozawa S, Suzuki K, Kaniwa N, Sawada J, Hamaguchi T, Yamamoto N, et al. (2007) Irinotecan pharmacokinetics/pharmacodynamics and UGT1A genetic polymorphisms in Japanese: roles of UGT1A1*6 and *28. *Pharmacogenet Genomics* **17:**497–504.

Ramírez J, Liu W, Mirkov S, Desai AA, Chen P, Das S, Innocenti F, and Ratain MJ (2007) Lack of association between common polymorphisms in UGT1A9 and gene expression and activity. *Drug Metab Dispos* **35:**2149–2153.

Saeki M, Saito Y, Jinno H, Sai K, Ozawa S, Kurose K, Kaniwa N, Komamura K, Kotake T, Morishita H, et al. (2006) Haplotype structures of the UGT1A gene complex in a Japanese population. *Pharmacogenomics J* **6:**63–75.

Sai K, Saeki M, Saito Y, Ozawa S, Katori N, Jinno H, Hasegawa R, Kaniwa N, Sawada J, Komamura K, et al. (2004) UGT1A1 haplotypes associated with reduced glucuronidation and increased serum bilirubin in irinotecan-administered Japanese patients with cancer. *Clin Pharmacol Ther* **75:**501–515.

Saito Y, Maekawa K, Ozawa S, and Sawada J (2007) Genetic polymorphisms and haplotypes of major drug metabolizing enzymes in East Asians and their comparison with other ethnic populations. *Curr Pharmacogenomics* **5:**49–78.

Sandanaraj E, Jada SR, Shu X, Lim R, Lee SC, Zhou Q, Zhou S, Goh BC, and Chowbay B (2008) Influence of UGT1A9 intronic I399C>T polymorphism on SN-38 glucuronidation in Asian cancer patients. *Pharmacogenomics J* **8:**174–185.

Smith NF, Figg WD, and Sparreboom A (2006) Pharmacogenetics of irinotecan metabolism and transport: an update. *Toxicol In Vitro* **20:**163–175.

Sugatani J, Yamakawa K, Yoshinari K, Machida T, Takagi H, Mori M, Kakizaki S, Sueyoshi T, Negishi M, and Miwa M (2002) Identification of a defect in the UGT1A1 gene promoter and its association with hyperbilirubinemia. *Biochem Biophys Res Commun* **292:**492–497.

Tukey RH and Strassburg CP (2000) Human UDP-glucuronosyltransferases: metabolism, expression, and disease. *Annu Rev Pharmacol Toxicol* **40:**581–616.

Address correspondence to: Dr. Yoshiro Saito, Division of Functional Biochemistry and Genomics, National Institute of Health Sciences, 1-18-1 Kamiyoga, Setagaya-ku, Tokyo 158-8501, Japan. E-mail: yoshiro@nihs.go.jp

Circulating Endothelial Cells in Non-small Cell Lung Cancer Patients Treated with Carboplatin and Paclitaxel

Makoto Kawaishi, MD, Yutaka Fujiwara, MD,† Tomoya Fukui, MD,* Terufumi Kato, MD,* Kazuhiko Yamada, MD,† Yuichiro Ohe, MD, PhD,† Hideo Kunitoh, MD, PhD,† Ikuo Sekine, MD, PhD,† Noboru Yamamoto, MD, PhD,† Hiroshi Nokihara, MD, PhD,† Takeshi Watabe, PhD,‡ Yuji Shimoda, PhD,‡ Tokuzo Arao, MD, PhD,§ Kazuto Nishio, MD, PhD,§ Tomohide Tamura, MD† and Fumiaki Koizumi, MD, PhD**

Introduction: Circulating endothelial cells (CECs) increase in cancer patients and play an important role in tumor neovascularization.
Methods: This study was designed to investigate the role of CEC as a marker for predicting the effectiveness of a carboplatin plus paclitaxel based first line chemotherapy in advanced non-small cell lung cancer (NSCLC).
Results: The CEC count in 4 ml of peripheral blood before starting chemotherapy (baseline value) was significantly higher in NSCLC patients, ranging from 32 to 4501/4 ml (n = 31, mean ± SD = 595 ± 832), than in healthy volunteers (n = 53, 46.2 ± 86.3). We did not detect a significant correlation between the CEC count and estimated tumor volume. CECs were significantly decreased by chemotherapy as compared with pretreatment values (175.6 ± 24 and 173.0 ± 24, day +8, +22, respectively). We investigated the correlation between baseline CEC and the clinical effectiveness of chemotherapy. CEC values are significantly higher in patients with clinical benefit (partial response and stable disease, 516 ± 458, 870.8 ± 1215, respectively) than in progressive disease patients (211 ± 150). Furthermore, a statistically significant decrease in CECs, on day 22, was observed only in patients with partial response. Patients who had a baseline CEC count greater than 400/4 ml showed a longer progression-free survival (>400, 271 days [range: 181–361] versus <400, 34 [range: 81–186], p = 0.019).
Conclusion: CEC is suggested to be a promising predictive marker of the clinical efficacy of the CBDCA plus paclitaxel regimen in patients with NSCLC.

Key Words: Circulating endothelial cell, NSCLC, Chemotherapy.

(*J Thorac Oncol.* 2009;4: 208–213)

Angiogenesis plays a critical role in the growth and metastasis of solid tumors.[1] The clinical importance of angiogenesis in human tumors has been demonstrated by several reports indicating a positive relationship between the blood vessel density in the tumor mass and poor prognosis, i.e., survival, in patients with various types of cancers including non-small cell lung cancer (NSCLC).[2–6] Furthermore, Natsume et al.[7] reported the antitumor activities of anticancer agents to be less active against vascular endothelial growth factor-secreting cells (SBC-3/VEGF), in vivo as compared with its mock transfectant (SBC-3/Neo). In recent years, antiangiogenic agents have also been demonstrated to be active against a variety of malignancies, including lung, colorectal, and renal cancer.[8–10] Thus, angiogenesis is a promising target for cancer treatment and is related to the prognosis and efficacy of these drugs, though the tumor vessel biomarkers which predict the effectiveness of antiangiogenic agents and other anticancer agents are not always useful and have not become well-established.

Circulating endothelial cells (CECs) have been recognized as a useful biomarker for vascular damage. CECs are increased in cardiovascular disease, vasculitis, infectious disease, and various cancers.[11–14] Recently, CECs were found to be more numerous and viable in cancer patients than in healthy subjects.[14,15] Furthermore, elevated CECs in cancer patients were found to be nearly normalized when the tumor was removed surgically or with chemotherapy.[15] Therefore, most CECs are considered to be disseminated tissue endothelial cells in the tumors and the CEC number may reflect the extent of tumor angiogenesis. Indeed, the CEC level has been demonstrated to correlate with the plasma level of VEGF, one of the pivotal factors promoting tumor angiogenesis.[15] Mancuso et al. reported that CEC kinetics and viability are promising predictors of the response to chemotherapy with antiangiogenic activity in patients with advanced breast cancer.[16] Thus, CEC is likely to be a useful marker for predicting the effectiveness of chemotherapy as a noninvasive angiogenesis marker.

NSCLC is the leading cause of cancer-related death worldwide. NSCLC accounts for approximately 50% of patients presenting with unresectable advanced stage,[17] and platinum-based chemotherapy offers only a small improve-

*Shien-Lab; †Medical Oncology, National Cancer Center Hospital, Chuo-ku, Tokyo, Japan; ‡Center for Molecular Biology and Cytogenetics, SRL Inc., Shinmachi, Hino-shi, Tokyo; and §Department of Genome Biology, Kinki University School of Medicine, Osaka-Sayama-shi, Osaka, Japan.
Disclosure: The authors declare no conflicts of interest.
Address for correspondence: Fumiaki Koizumi, MD, PhD, Shien-Lab, National Cancer Center Hospital, 5-1-1 Tsukiji, Chuo-ku, Tokyo, Japan. E-mail: fkoizumi@gan2.res.ncc.go.jp
Copyright © 2009 by the International Association for the Study of Lung Cancer
ISSN: 1556-0864/09/0402-0208

Copyright © 2009 by the International Association for the Study of Lung Cancer.

ment in survival with advanced NSCLC.[18,19] Over the past decade, several new agents against NSCLC have become available, including the taxanes, gemcitabine, vinorelbine, and irinotecan. The combination of platinum and these new agents has resulted in a high response rate and prolonged survival compared with older chemotherapy regimens (e.g., vindesine, mitomycin, ifosfamide, with cisplatin). Therefore, these regimens are considered standard chemotherapy for advanced NSCLC.[20–26] Although new agents have different mechanisms of action, these combination regimens have not been administered based on the biologic characteristics of each tumor.

Paclitaxel inhibits several endothelial cell functions in vitro such as proliferation, migration, morphogenesis, and metalloprotease production.[27–29] These activities result in antiangiogenic activity in in vivo xenograft models.[27,30] Interestingly, human endothelial cells are more sensitive to paclitaxel than other cellular types.[29] We hypothesized that the CEC value is associated with tumor neovascularization, which is one of the targets of paclitaxel. In the present study, we investigated whether the CEC count at baseline is associated with the effectiveness of the CDDP plus paclitaxel regimen in patients with advanced-stage NSCLC.

TABLE 1. Baseline Characteristics of the Patients

Characteristic	$N = 31$ No. (%)
Gender	
Male	17 (55)
Female	14 (45)
Median age (yr)	60
Range	43–71
ECOG performance status	
0	18 (58)
1	13 (42)
Stage	
IIIA	2 (6)
IIIB	7 (23)
IV	22 (71)
Histology	
Adenocarcinoma	23 (74)
Squamous cell carcinoma	4 (13)
Others	4 (13)

MATERIALS AND METHODS

Patients

Patients with histologically or cytologically documented advanced NSCLC were eligible for this study. Each patient was required to meet the following criteria: (1) no prior treatment including chemotherapy, surgery, irradiation, or any fluid drainage; (2) no prior general anesthesia for diagnostic procedures including mediastinoscopy or thoracoscopy; (3) no concomitant diseases including ischemic heart diseases, systemic vasculitis, pulmonary hypertension, or serious complications including infectious disease or diabetes; (4) written informed consent. The trial document was approved by the institutional review board. The clinical characteristics of the patients are shown in Table 1.

Treatment Schedule and Response Evaluation

All patients were treated according to the following chemotherapeutic regimen: paclitaxel at 200 mg/m^2 over a 3-hour period followed by carboplatin at a dose with an area under the curve of 6 on day 1, repeated every 3 weeks. The treatment was repeated for three or more cycles unless the patients met the criteria for progressive disease (PD) or experienced unacceptable toxicity.

The major axis (a) and minor axis (b) of the tumor mass in each patient were measured with computed tomography. Estimated tumor volume (ETV) was calculated using the following formula; ETV = $4/3 \times \pi$ (a/2 × b/2) × (a/2 + b/2)/2. Computed tomography examinations were performed before treatment and with every one or two cycles of chemotherapy. Response was evaluated according to the RECIST, and tumor markers were excluded from the criteria.[31]

Assay for CEC

Blood samples from NSCLC patients and healthy volunteers were drawn into a 10-ml Cellsave Preservative Tube (Immunicon Corp. Huntingdon Valley, PA) for CEC enumeration. The CEC protocol used was approved by the Institutional Review Board and written informed consent was obtained from each subject. Samples from NSCLC were obtained before (baseline) and 8 and 22 days after starting chemotherapy. Samples were kept at room temperature and processed within 42 hours after collection. All evaluations were performed without knowledge of the clinical status of the patients. The CellTracks system (Immunicon Corp) which consists of CellTracks AutoPrep system and the CellSpotter Analyzer system was used for endothelial cell enumeration.[32,33] In this system, CD146+/DAPI+/CD105-PE+/CD45APC- cells are defined as CECs. Briefly, cells which express CD146 were immunomagnetically captured using ferrofluids coated with CD146 antibodies. The enriched cells were then labeled with the nuclear dye 4V,6-diamidino-2-phenylindole (DAPI), CD105 antibodies conjugated to phycoerythrin (CD105-PE), and the pan-leukocyte antibody CD45 conjugated to allophycocyanin (CD45-APC). In this system, the CD146-enriched, fluorescently labeled cells were identified as CECs when the cells exhibited the DAPI+/CD105+/CD45- phenotype. We performed CEC enumeration twice, using the same sample, and calculated the mean value.

Statistical Analyses

This study was carried out as exploratory research for detecting CECs from NSCLC patients. The number of enrolled patients was therefore not precalculated. Spearman's correlation analysis was performed to investigate the correlation between CEC count and ETV. Between-group comparisons were made using the t test. The association between CEC count and progression free survival (PFS) was estimated using the Kaplan-Meier method. The log-rank test was used to assess the survival difference between strata. Differences were considered statistically significant at $p < 0.05$.

Copyright © 2009 by the International Association for the Study of Lung Cancer

Copyright © 2009 by the International Association for the Study of Lung Cancer.

RESULTS

Patient Characteristics

A total of 32 patients were enrolled in the study between August 2005 and March 2006 (Table 1). One patient withdrew consent to participate. Table 1 summarizes the characteristics of the study population. The median age of the patients was 60 years (range, 43–71). The histologic and/or cytologic diagnosis was adenocarcinoma in 23 patients (74.2%), squamous cell carcinoma in 4 (12.9%), and unclassified NSCLC in 4 (12.9%). There were 17 males (54.8%). The clinical stage was IIIA in 2 patients (6.5%), IIIB in 7 (22.6%), and IV in 22 (71.0%).

Ninety-two CEC samples from 31 patients (three samples per patient) were obtained and analyzed. One sample, obtained 22 days after treatment, was not examined because of inadequate collection.

Quantification of CEC

In 31 advanced NSCLC patients, CECs ranged from 32 to 4501 cells/4.0 ml of blood, mean ± SD = 595 ± 832 at baseline. CEC counts were elevated in a large portion of patients with NSCLC as compared with healthy volunteers (n = 53, mean ± SD = 46.2 ± 86.3/4 ml). Case 21 had an exceptionally high CEC count (4501 at baseline). We did not detect a significant correlation between the CEC count and ETV in the 28 assessable patients (p = 0.84, Figure 1). The analysis of CECs during the first course of treatment showed CEC levels to be reduced by CBDCA plus paclitaxel chemotherapy as compared with pretreatment values (176 ± 141 at 8 days and 173 ± 189 at 22 days after treatment) (Figure 2). These reductions were significant (p = 0.011 on day 8 and p = 0.04 on day 22), but there was no significant difference between CEC amounts on day 8 versus day 22 (p = 0.476). There was no difference in the amount of CEC at baseline when patients were subgrouped according to characteristics, such as sex, smoking history, histologic type, and clinical stage. Furthermore, there was no correlation of CEC amounts with the blood examination data (e.g., number of white blood cells, neutrophils, lymphocytes, hemoglobin, platelets, albumin, LDH, CRP, CEA, CYFRA).

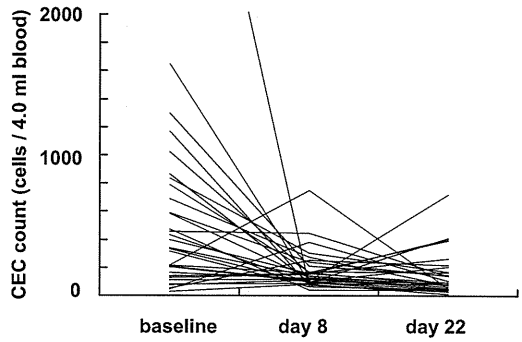

	baseline	day 8	day 22
mean ± SD	595± 832	176± 141 *	173 ± 189 *

FIGURE 2. Circulating endothelial cell (CEC) levels during the first course of CDDP plus paclitaxel chemotherapy. *p < 0.05 versus values at baseline.

CEC Amounts and Objective Tumor Response to Chemotherapy

Thirteen (41.9%) of the 31 patients who received carboplatin and paclitaxel therapy showed a partial response (PR) and 12 (38.7%) showed stable disease (SD). The other 6 patients (19.4%) showed PD. The amounts of CEC at baseline in the patients who showed PR and SD were 516 ± 458/4 ml and 871 ± 1215/4 ml, respectively, and these values were significantly higher than in PD patients (211 ± 150/4 ml, p = 0.023 and p = 0.044, respectively) (Figure 3*A*). Although CEC decrements during chemotherapy were observed in all three subgroups, the extent of the decrements tended to be greater in

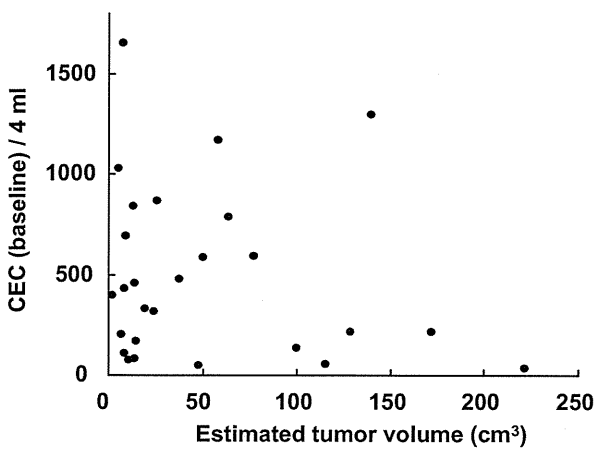

FIGURE 1. Scatter plot analysis to determine the correlation between the number of circulating endothelial cell (CEC) and estimated tumor volume (ETV). ETV is calculated with computed tomography (CT) examination. Case 21 is not included.

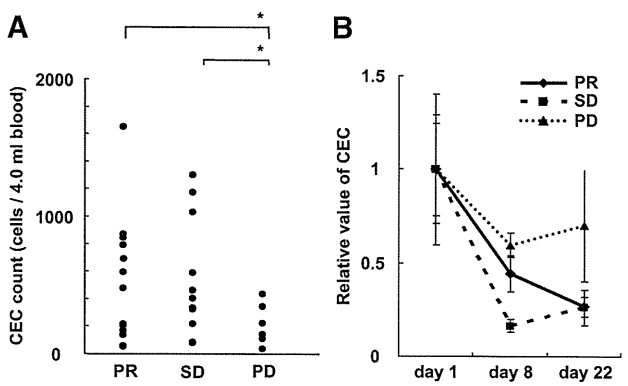

FIGURE 3. *A*, Comparison of circulating endothelial cell (CEC) amount at baseline in non-small cell lung cancer (NSCLC) patients with different clinical responses to CBDCA plus paclitaxel chemotherapy. *p < 0.05 versus values of patients with progressive disease (PD). Case 21 is not included. *B*, Relative change in CEC amount in patients with partial response (PR), stable disease (SD), and PD.

Copyright © 2009 by the International Association for the Study of Lung Cancer

Copyright © 2009 by the International Association for the Study of Lung Cancer.

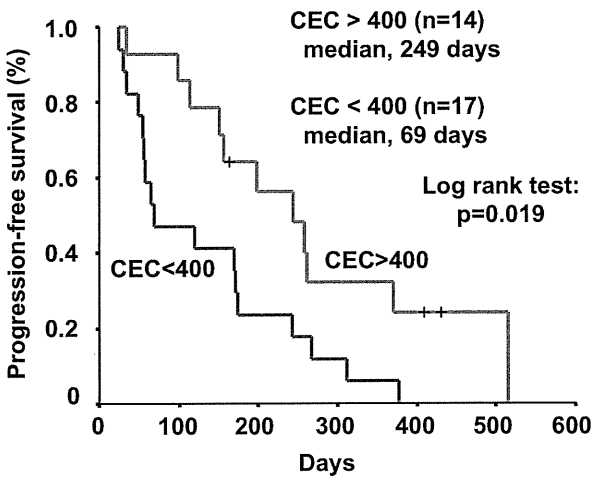

FIGURE 4. Progression-free-survival according to circulating endothelial cell (CEC) count at baseline. The median duration of progression-free survival was greater in patients whose CEC count exceeded 400 (median, 244 days) than in patients whose CEC count was less than 400 (69 days).

patients with PR and SD than in those with PD (Figure 3*B*). In the subgroup analysis, a significant decrease in CECs was observed on day 22 only in PR patients ($p = 0.018$).

CEC Amounts and PFS

For all 31 patients, the median PFS was 154 days (range, 81–361 days). Univariate analysis indicated that patients who had a CEC count of more than 400/4 ml at baseline showed a significantly improved PFS ($n = 14$, median; 244 days) (Log-rank test, $p = 0.019$, Figure 4). A CEC count below 400 at baseline was associated with a poorer PFS ($n = 17$, median; 69 days). The CEC count did not exceed the value of 400/4 ml in any of the healthy volunteers. When we compared the patients whose CEC counts exceeded 200 with those whose counts were less than 200, a consistent difference in PFS was observed between the two groups (>200; $n = 22$, median 227, <200; $n = 9$, median 116, $p < 0.039$).

DISCUSSION

In the present study, we investigated the number of CEC during the first course of CBDCA plus paclitaxel chemotherapy. To our knowledge, this is the first report of CEC in NSCLC patients before treatment. Our findings demonstrated CEC counts in advanced NSCLC at baseline level to be much higher than those in healthy subjects (595 ± 832/4.0 ml versus 32.6 ± 29.5/4.0 ml). Because the NSCLC patients had not yet received anticancer therapy, these increased CECs are likely to be mostly derived from the tumor site. In a previous study, it was found that the amounts of CECs correlate strongly with tumor volume in vivo in an animal model[34]. Nevertheless, we did not find a significant correlation between CECs and ETV. Because the number of CECs could be influenced by many factors related to tumor vasculature, neovascularization, and localization of the tumor, our failure to identify a strong correlation in this study is not surprising. We were also unable to detect a significant direct correlation between CEC amounts and various blood examination data including tumor markers such as CEA and CYFRA. It is unclear at present what biologic characteristics of the tumor or clinical features the CEC number most closely reflects as a biomarker. Mancuso et al. reported that CECs are strongly associated with plasma levels of VCAM-1 and VEGF in breast cancer and lymphoma patients.[15,34] Because VCAM-1 and VEGF are crucial factors for tumor angiogenesis, the variability in CEC values among NSCLC patients might indicate a difference in the neovascularization of each tumor.

We were further able to demonstrate that elevated CECs decreased dramatically after CBDCA plus paclitaxel treatment, but did not reach the level of healthy subjects. Decreased CEC values did not rise again during the first cycle of chemotherapy. Although myelosupression was observed on day 8 and recovered on day 22 in many patients (data not shown), CEC kinetics do not parallel those of WBC, indicating that CEC kinetics might not be influenced by myelopoiesis. Several clinical studies in the field measuring CEC found chemotherapy to be associated with either an increase or a decrease in CECs.[35–39] The different tumor types, stages, prior therapy or not, the anticancer drugs used, measuring points and quantification methods of CEC might have influenced the CEC results after treatment. In the present study, the pretreatment CEC value was much higher than that in lung cancer with metastasis (mean ± SD = 146 ± 270/4 ml), as reported elsewhere.[33] Although the details of the prior therapy in patients with metastatic carcinoma were not provided,[33] chemotherapy can eventually decrease the CEC count.

Schiller et al. compared four standard chemotherapy regimens, cisplatin plus paclitaxel, cisplatin plus gemcitabine, cisplatin plus docetaxel, and carboplatin plus paclitaxel and found no significant difference in survival.[25] Despite the different modes of action of each nonplatinum agent against tumors and different biologic characteristics of each tumor, we could not select the regimen based on these characteristics. In our small study, the patients with PR/SD and longer PFS had higher baseline CEC values. Therefore, it seems that the baseline CEC count is a promising predictor of clinical response to the CBDCA plus paclitaxel regimen and survival in advanced NSCLC. If CEC is a marker for angiogenesis and reflects tumor neovascularization, it is likely that a high CEC is associated with a poor prognosis and lower effectiveness of antiangiogenic therapy. Paclitaxel and docetaxel are categorized as mitotic spindle agents with potent antiangiogenic properties.[27–30] This is why a paclitaxel based regimen might be more effective against tumors with high CEC values. Nevertheless, CEC counts have also been reported to be increased in several clinical syndromes, such as cardiovascular diseases, infectious diseases, and vasculitides.[11–13] The CEC counts in patients with vasculitides have been reported to be dozens of fold higher than those in healthy subjects,[12] therefore, we have to consider the patient condition carefully while interpreting the CEC counts in individual patients, although there were no patients with vasculitis in the present study. Further clinical investigation, with a similar approach, including other nonplatinum anticancer agents, such as

Copyright © 2009 by the International Association for the Study of Lung Cancer

Copyright © 2009 by the International Association for the Study of Lung Cancer.

CDDP plus gemcitabine, is essential for the clinical application of CEC for made-to-order chemotherapy in NSCLC.

Antiangiogenic therapy targeting the VEGF pathway such as bevacizumab and VEGFR inhibitors have shown promise in the treatment of solid tumors.[8,39] These agents inhibit endothelial cells through inhibition of the VEGF pathway. It was recently demonstrated that the addition of bevacizumab to CBDCA plus paclitaxel in advanced NSCLC patients produces a significant survival benefit as compared with chemotherapy alone.[40] Considering the outstanding clinical trial and our present study, it would be of great interest to investigate the role of CEC in this regimen.

In conclusion, CECs were measured in NSCLC patients before treatment. Our small clinical study indicates that the CEC count at baseline is a potential biomarker for predicting the response to chemotherapy and PFS, but further clinical evaluation is needed. In the near future, we will start a clinical investigation, using a similar approach, to examine other chemotherapeutic regimens.

ACKNOWLEDGEMENTS

This study was supported in part by a Grant-in-Aid for the 3rd Term Comprehensive 10-year Strategy for Cancer Control from the Ministry of Health, Welfare and Labour, Japan.

REFERENCES

1. Folkman J. Anti-angiogenesis: new concept for therapy of solid tumors. *Ann Surg* 1972;175:409–416.
2. Gasparini G, Harris AL. Clinical importance of the determination of tumor angiogenesis in breast carcinoma: much more than a new prognostic tool. *J Clin Oncol* 1995;13:765–782.
3. Dickinson AJ, Fox SB, Persad RA, Hollyer J, Sibley GN, Harris AL. Quantification of angiogenesis as an independent predictor of prognosis in invasive bladder carcinomas. *Br J Urol* 1994;74:762–766.
4. Takahashi Y, Kitadai Y, Bucana CD, Cleary KR, Ellis LM. Expression of vascular endothelial growth factor and its receptor, KDR, correlates with vascularity, metastasis, and proliferation of human colon cancer. *Cancer Res* 1995;55:3964–3968.
5. Williams JK, Carlson GW, Cohen C, Derose PB, Hunter S, Jurkiewicz MJ. Tumor angiogenesis as a prognostic factor in oral cavity tumors. *Am J Surg* 1994;168:373–380.
6. Koukourakis MI, Giatromanolaki A, Thorpe PE, et al. Vascular endothelial growth factor/KDR activated microvessel density versus CD31 standard microvessel density in non-small cell lung cancer. *Cancer Res* 2000;60:3088–3095.
7. Natsume T, Watanabe J, Koh Y, et al. Antitumor activity of TZT-1027 (Soblidotin) against vascular endothelial growth factor-secreting human lung cancer in vivo. *Cancer Sci* 2003;94:826–833.
8. Hurwitz H, Fehrenbacher L, Novotny W, et al. Bevacizumab plus irinotecan, fluorouracil, and leucovorin for metastatic colorectal cancer. *N Engl J Med* 2004;350:2335–2342.
9. Yang JC, Haworth L, Sherry RM, et al. A randomized trial of bevacizumab, an anti-vascular endothelial growth factor antibody, for metastatic renal cancer. *N Engl J Med* 2003;349:427–434.
10. Johnson DH, Fehrenbacher L, Novotny WF, et al. Randomized phase II trial comparing bevacizumab plus carboplatin and paclitaxel with carboplatin and paclitaxel alone in previously untreated locally advanced or metastatic non-small-cell lung cancer. *J Clin Oncol* 2004;22:2184–191.
11. Mutin M, Canavy I, Blann A, Bory M, Sampol J, Dignat-George F. Direct evidence of endothelial injury in acute myocardial infarction and unstable angina by demonstration of circulating endothelial cells. *Blood* 1999;93:2951–2958.
12. Woywodt A, Streiber F, De Groot K, Regelsberger H, Haller H, Haubitz M. Circulating endothelial cells as markers for ANCA associated small-vessel vasculitis. *Lancet* 2003;361:206–210.
13. Mutunga M, Fulton B, Bullock R, et al. Circulating endothelial cells in patients with septic shock. *Am J Respir Crit Care Med* 2001;163:195–200.
14. Beerepoot LV, Mehra N, Vermaat JS, Zonnenberg BA, Gebbink MF, Voest EE. Increased levels of viable circulating endothelial cells are an indicator of progressive disease in cancer patients. *Ann Oncol* 2004;15:139–145.
15. Mancuso P, Burlini A, Pruneri G, Goldhirsch A, Martinelli G, Bertolini F. Resting and activated endothelial cells are increased in the peripheral blood of cancer patients. *Blood* 2001;97:3658–3661.
16. Mancuso P, Colleoni M, Calleri A, et al. Circulating endothelial-cell kinetics and viability predict survival in breast cancer patients receiving metronomic chemotherapy. *Blood* 2006;108:452–459.
17. Bülzebruck H, Bopp R, Drings P, et al. New aspects in the staging of lung cancer. Prospective validation of the International Union Against Cancer TNM classification. *Cancer* 1992;70:1102–1110.
18. Grilli R, Oxman AD, Julian JA. Chemotherapy for advanced non-small-cell lung cancer: how much benefit is enough? *J Clin Oncol* 1993;11:1866–1872.
19. Non-small Cell Lung Cancer Collaborative Group. Chemotherapy in non-small cell lung cancer: a meta-analysis using updated data on individual patients from 52 randomised clinical trials. *BMJ* 1995;311:899–909.
20. Kubota K, Watanabe K, Kunitoh H, et al. Phase III randomized trial of docetaxel plus cisplatin versus vindesine plus cisplatin in patients with stage IV non-small cell lung cancer: the Japanese Taxotere Lung Cancer Study Group. *J Clin Oncol* 2004;22:254–261.
21. Le Chevalier T, Brisgand D, Douillard JY, et al. Randomized study of vinorelbine and cisplatin versus vindesine and cisplatin versus vinorelbine alone in advanced non-small cell lung cancer: results of a European multicenter trial including 612 patients. *J Clin Oncol* 1994;12:360–367.
22. Belani CP, Lee JS, Socinski MA, et al. Randomized phase III trial comparing cisplatin-etoposide to carboplatin-paclitaxel in advanced or metastatic non-small cell lung cancer. *Ann Oncol* 2005;16:1069–1075.
23. Yana T, Takada M, Origasa H, et al. New chemotherapy agent plus platinum for advanced non-small cell lung cancer: a meta-analysis. *Proc Am Soc Clin Oncol* 2002;21:328a.
24. Baggstrom MQ, Stinchcombe TE, Fried DB, Poole C, Hensing TA, Socinski MA. Third-generation chemotherapy agents in the treatment of advanced non-small cell lung cancer: a meta-analysis. *J Thorac Oncol* 2007;2:845–853.
25. Schiller JH, Harrington D, Belani CP, et al; Eastern Cooperative Oncology Group. Comparison of four chemotherapy regimens for advanced non-small-cell lung cancer. *N Engl J Med* 2002;346:92–98.
26. Ohe Y, Ohashi Y, Kubota K, et al. Randomized phase III study of cisplatin plus irinotecan versus carboplatin plus paclitaxel, cisplatin plus gemcitabine, and cisplatin plus vinorelbine for advanced non-small-cell lung cancer: Four-Arm Cooperative Study in Japan. *Ann Oncol* 2007;18:317–323.
27. Belotti D, Vergani V, Drudis T, et al. The microtubule-affecting drug paclitaxel has antiangiogenic activity. *Clin Cancer Res* 1996;2:1843–1849.
28. Hayot C, Farinelle S, De Decker R, et al. In vitro pharmacological characterizations of the anti-angiogenic and anti-tumor cell migration properties mediated by microtubule-affecting drugs, with special emphasis on the organization of the actin cytoskeleton. *Int J Oncol* 2002;21:417–425.
29. Wang J, Lou P, Lesniewski R, Henkin J. Paclitaxel at ultra low concentrations inhibits angiogenesis without affecting cellular microtubule assembly. *Anticancer Drugs* 2003;14:13–19.
30. Vacca A, Ribatti D, Iurlaro M, et al. Docetaxel versus paclitaxel for antiangiogenesis. *J Hematother Stem Cell Res* 2002;11:103–118.
31. Therasse P, Arbuck SG, Eisenhauer EA, et al. New guidelines to evaluate the response to treatment in solid tumors. European Organization for Research and Treatment of Cancer, National Cancer Institute of the United States, National Cancer Institute of Canada. *J Natl Cancer Inst* 2000;92:205–216.
32. Smirnov DA, Foulk BW, Doyle GV, Connelly MC, Terstappen LW, O'Hara SM. Global gene expression profiling of circulating endothelial cells in patients with metastatic carcinomas. *Cancer Res* 2006;66:2918–2922.
33. Rowand JL, Martin G, Doyle GV, et al. Endothelial cells in peripheral blood of healthy subjects and patients with metastatic carcinomas. *Cytometry A* 2007;71A:105–114.
34. Mancuso P, Calleri A, Cassi C, et al. Circulating endothelial cells as a novel marker of angiogenesis. *Adv Exp Med Biol* 2003;522:83–97.

Copyright © 2009 by the International Association for the Study of Lung Cancer

Copyright © 2009 by the International Association for the Study of Lung Cancer.

35. Beaudry P, Force J, Naumov GN, et al. Differential effects of vascular endothelial growth factor receptor-2 inhibitor ZD6474 on circulating endothelial progenitors and mature circulating endothelial cells: implications for use as a surrogate marker of antiangiogenic activity. *Clin Cancer Res* 2005;11:3514–3522.
36. Fürstenberger G, von Moos R, Lucas R, et al. Circulating endothelial cells and angiogenic serum factors during neoadjuvant chemotherapy of primary breast cancer. *Br J Cancer* 2006;94:524–531.
37. Rademaker-Lakhai JM, Beerepoot LV, Mehra N, et al. Phase I pharmacokinetic and pharmacodynamic study of the oral protein kinase C beta-inhibitor enzastaurin in combination with gemcitabine and cisplatin in patients with advanced cancer. *Clin Cancer Res* 2007;13:4474–4481.
38. McAuliffe JC, Trent JC. Biomarkers in gastrointestinal stromal tumor: should we equate blood-based pharmacodynamics with tumor biology and clinical outcomes? *Clin Cancer Res* 2007;13:2643–2650.
39. Hanrahan EO, Heymach JV. Vascular endothelial growth factor receptor tyrosine kinase inhibitors vandetanib (ZD6474) and AZD2171 in lung cancer. *Clin Cancer Res* 2007;13:S4617–S4622.
40. Sandler A, Gray R, Perry MC, et al. Paclitaxel-carboplatin alone or with bevacizumab for non-small-cell lung cancer. *N Engl J Med* 2006;355:2542–2550; 2007;356:318.

Copyright © 2009 by the International Association for the Study of Lung Cancer

Copyright © 2009 by the International Association for the Study of Lung Cancer.

Drug Metab. Pharmacokinet. 24 (1): 118–126 (2009).

SNP Communication

Genetic Variations and Haplotype Structures of the Glutathione *S*-transferase Genes, *GSTT1* and *GSTM1*, in a Japanese Patient Population

Naoko TATEWAKI[1], Keiko MAEKAWA[1,2,*], Noriko KATORI[1,3], Kouichi KUROSE[1,4], Nahoko KANIWA[1,4], Noboru YAMAMOTO[5], Hideo KUNITOH[5], Yuichiro OHE[5], Hiroshi NOKIHARA[5], Ikuo SEKINE[5], Tomohide TAMURA[5], Teruhiko YOSHIDA[6], Nagahiro SAIJO[7], Yoshiro SAITO[1,2] and Jun-ichi SAWADA[1,2]

[1]*Project team for Pharmacogenetics, National Institute of Health Sciences, Tokyo, Japan*
[2]*Division of Functional Biochemistry and Genomics, National Institute of Health Sciences, Tokyo, Japan*
[3]*Division of Drugs, National Institute of Health Sciences, Tokyo, Japan*
[4]*Division of Medicinal Safety Science, National Institute of Health Sciences, Tokyo, Japan*
[5]*Thoracic Oncology Division, National Cancer Center Hospital, National Cancer Center, Tokyo, Japan*
[6]*Genetics Division, National Cancer Center Research Institute, National Cancer Center, Tokyo, Japan*
[7]*Deputy Director, National Cancer Center Hospital East, Kashiwa, Japan*

Full text of this paper is available at http://www.jstage.jst.go.jp/browse/dmpk

Summary: Glutathione *S*-transferases (GSTs) play a vital role in phase II biotransformation of many synthetic chemicals including anticancer drugs. Deletion polymorphisms in *GSTT1* and *GSTM1* are reportedly associated, albeit controversial, with an increased risk in cancer as well as with altered responses to chemotherapeutic drugs. In this study, to elucidate the haplotype structures of *GSTT1* and *GSTM1*, genetic variations were identified in 194 Japanese cancer patients who received platinum-based chemotherapy. Homozygotes for deletion of *GSTT1* (*GSTT1*0/*0* or null) and *GSTM1* (*GSTM1*0/*0* or null) were found in 47.4% and 47.9% of the patients, respectively, while 23.2% of the patients had both *GSTT1* null and *GSTM1* null genotypes. From homozygous (+/+) and heterozygous (*0/+) patients bearing *GSTT1* and *GSTM1* genes, six single nucleotide polymorphisms (SNPs) for *GSTT1* and 23 SNPs for *GSTM1* were identified. A novel SNP in *GSTT1*, 226C>A (Arg76Ser), and the known SNP in *GSTM1*, 519C>G (Asn173Lys, **B*), were found at frequencies of 0.003 and 0.077, respectively. Using the detected variations, *GSTT1* and *GSTM1* haplotypes were identified/inferred. Three and six common haplotypes (N≥10) in *GSTT1* and *GSTM1*, respectively, accounted for most (>95%) inferred haplotypes. This information would be useful in pharmacogenomic studies of xenobiotics including anticancer drugs.

Keywords: *GSTT1*; *GSTM1*; nonsynonymous SNP; haplotype; haplotype-tagging SNP

Introduction

Glutathione *S*-transferases (GSTs) (EC 2.5.1.18) are dimeric phase II metabolic enzymes that mainly catalyze conjugation of reduced glutathione (GSH) with a variety of electrophilic compounds including carcinogens, therapeutic drugs and environmental toxins as well as endogenous substances.[1)] In addition, GSTs possess selenium-independent GSH peroxidase activity to reduce organic hydroperoxides, and therefore, play significant roles in detoxification, occasionally toxification, and cellular protection against oxidative stress.[2)] Noncatalytical-

Received; May 11, 2008, Accepted; August 20, 2008
**To whom correspondence should be addressed:* Keiko MAEKAWA, Ph.D., *Division of Functional Biochemistry and Genomics, National Institute of Health Sciences, 1-18-1 Kamiyoga, Setagaya-ku, Tokyo 158-8501, Japan. Tel. +81-3-3700-9453, Fax. +81-3-5717-3832, E-mail: maekawa@nihs.go.jp*
On April 28th, 2008, the novel variations described in this paper were not found in the Japanese Single Nucleotide Polymorphisms (JSNP) (http://snp.ims.u-tokyo.ac.jp/), dbSNP in the National Center for Biotechnology Information (http://www.ncbi.nlm.nih.gov/SNP/) or SNP500Cancer Database (http://snp500cancer.nci.nih.gov/).
This study was supported in part by the Program for the Promotion of Fundamental Studies in Health Sciences and in part by the Health and Labor Sciences Research Grants from the Ministry of Health, Labor and Welfare.

ly, GSTs modulate signaling pathways by interacting with protein kinases[3] and by binding numerous ligands for nuclear hormone receptors.[4]

Human GSTs are composed of three main families: cytosolic, mitochondrial and microsomal (or membrane-bound). The cytosolic family, which is principally involved in biotransformation of toxic xenobiotics, contains at least 17 genes subdivided into seven separate classes designated alpha, mu, pi, sigma, theta, zeta, and omega.[5,6] Increasing numbers of GST genes are identified as polymorphic.

The θ-class enzyme GSTT1 and the μ-class enzyme GSTM1 exhibit gene deletion polymorphisms (*GSTT1*0* and *GSTM1*0*, respectively).[7] The null genotype of *GSTT1* (*GSTT1*0/*0*) is found in 15–40% of Caucasians and 50–60% of Asians.[7] On the other hand, about half of both Japanese and Caucasians and 30% of Africans are homozygous for the *GSTM1* deletion (*GSTM1*0/*0*).[7] In intact *GSTM1*, alleles **A* and **B* are used to discriminate the single nucleotide polymorphism (SNP) with amino acid substitution (thereafter, nonsynonymous SNP), 519C>G (Asn173Lys) in exon 7, in which both alleles encode proteins that are catalytically identical for the substrates, 1-chloro-2,4-dinitrobenzene (CDNB), *trans*-4-phenyl-3-buten-2-one (tPBO) and 1,2-epoxy-3-(*p*-nitrophenoxy)propane (EPNP).[8] In addition, a tandem duplication in *GSTM1* associated with ultrarapid enzyme activity was observed in Saudi Arabians.[9] A gene-dose effect has been clearly established: that is, homozygously deleted (**0/*0*), heterozygously (**0/+*) and homozygously intact (*+/+*) *GST* genotypes correspond to non-, intermediate, and high conjugators, respectively.[10,11]

A large number of association studies on *GSTM1* and *GSTT1* null genotypes have been performed with inter-individual differences in susceptibility to environmental toxins, cancer and other diseases, and in the outcomes of anticancer treatments. Increased risk of lung, bladder, breast and colon cancers were observed in carriers of *GSTM1* or *GSTT1* null genotypes, while other studies have reported controversial findings.[5-7] As for response to anti-cancer drugs, pharmacodynamic correlations have been investigated, but the obtained results are inconsistent.[6] It should be pointed out that despite the possible gene-dose effect, most association studies were only focused on null genotypes of *GSTM1* and/or *GSTT1*. Therefore, in addition to nonconjugators, discrimination between high and intermediate conjugators would be valuable to evaluate the clinical relevance of these GST loci. Also, certain SNPs in the intact genes might affect either the expression of the gene or the activity of the encoded enzyme.

In this study, we first determined the deletion genotypes (**0/0*, **0/+*, and *+/+*) of *GSTM1* and *GSTT1* by conventional PCR and TaqMan real-time quantitative PCR for 194 Japanese cancer patients treated by platinum-based chemotherapy. Then, we resequenced the homozygous and heterozygous intact *GSTM1* and *GSTT1* genes. Lastly, linkage disequilibrium (LD) and haplotype analyses were performed using the detected SNPs.

Materials and Methods

Human genomic DNA samples: All 194 patients participating in this study were administered carboplatin or nedaplatin in combination with paclitaxel for treatment of various cancers (mainly non-small cell lung cancers) at the National Cancer Center. Genomic DNA was extracted from blood leukocytes from all subjects prior to the chemotherapy. The ethical review boards of the National Cancer Center and National Institute of Health Sciences approved this study. Written informed consent was obtained from all subjects.

Conventional PCR amplification of the *GSTT1* deletion junction: We used the genotyping assay described by Sprenger *et al.*,[10] in which 1460 (for **0* allele) and 466 bp (for exon 5 of the wild-type) PCR fragments were coamplified by multiplex PCR. PCR reactions were performed according to their method with minor modification.[10] Briefly, PCR mixtures contained 100 ng of genomic DNA, 0.2 μM each of the 4 primers reported previously, 0.2 mM each of four deoxynucleotide triphospates (dNTPs), and 0.75 units of HotStarTaq polymerase (Qiagen, Tokyo, Japan) in a 50 μl volume. The PCR conditions were 95°C for 15 min, followed by 30 cycles of 94°C for 30 sec, and 65°C for 1.5 min. PCR fragments were analyzed on 1% agarose gels with ethidium bromide in TAE buffer.

Conventional PCR amplification of *GSTM1*: We used the method of McLellan *et al.* (1997),[9] in which exons 3 to 5 of *GSTM1* were coamplified with β-globin as an internal standard by multiplex PCR. The PCR reactions were carried out according to their method[9] except that 100 ng of genomic DNA and 0.75 units of HotStarTaq polymerase (Qiagen) were used in a 50 μl total volume. The PCR conditions were 94°C for 15 min, followed by 30 cycles of 94°C for 48 sec, 62°C for 48 sec, and 72°C for 1.5 min, and then a final extension for 5 min at 72°C.

Quantitative real-time PCR for *GSTM1* and *GSTT1*: Quantitative real-time PCR using the TaqMan (5′-nuclease) assay system was carried out according to the method of Covault *et al.*,[12] in which the amounts of target *GSTM1* or *GSTT1* were quantified relative to those of the reference β-2-microglobulin (*B2M*) or cannabinoid receptor 1 (*CNR1*), respectively. Briefly, triplicate reactions were performed for 5 ng of genomic DNA used as a template in 1x TaqMan Universal PCR Master Mix with Amp Erase (50 μl) (Applied Biosystems, Foster City, CA, USA). The thermal cycling conditions were 50°C for 2 min and then 95°C for 10 min, followed by 40 cycles of

95 °C for 20 sec and 60 °C for 1 min with the 7500 Real-Time PCR System (Applied Biosystems).

***GSTT1* DNA sequencing:** The heterozygous and homozygous samples for *GSTT1* (**0/+* and *+/+*), the 5′-flanking region (up to 801 bp upstream from the translation start site), all 5 exons with their surrounding introns and the 3′-flanking region were amplified by PCR and directly sequenced. For the 1st round PCR, the reaction mixtures contained 25 ng of genomic DNA, 1.25 units of Ex-Taq (Takara Bio. Inc. Shiga, Japan), 0.2 mM dNTPs, and 0.2 μM primers listed in **Table 1**. The PCR conditions were 94 °C for 5 min, followed by 30 cycles of 94 °C for 30 sec, 60 °C for 1 min, and 72 °C for 2 min; and then a final extension for 7 min at 72 °C. The regions from 5′-flanking to exon 1 and from exon 4 to 3′-flanking were amplified separately by the nested PCR with Ex-Taq (1.25 units) and the primer sets (0.2 μM) listed in "2nd round PCR" of **Table 1**. The 2nd round PCR conditions were the same as described in the 1st round PCR. The 2nd round PCR products and the 1st round PCR products for exons 2 and 3 were then treated with a PCR Product Pre-Sequencing Kit (USB Co., Cleveland, OH, USA) and were directly sequenced on both strands using an ABI BigDye Terminator Cycle Sequencing Kit (Applied Biosystems) with the sequencing primers listed in **Table 1** (Sequencing column). Excess dye was removed by a DyeEx96 kit (Qiagen, Hilden, Germany). Eluates were analyzed on an ABI Prism 3730 DNA Analyzer (Applied Biosystems). All novel SNPs were confirmed by repeated sequencing of the PCR products generated by new genomic DNA amplifications. The genomic and cDNA sequences of *GSTT1* obtained from GenBank (NT_011520.11 and NM_000853.1, respectively) were used as reference sequences.

***GSTM1* DNA sequencing:** For samples with **0/+* and *+/+*, genetic variations were identified by resequencing. Particular attention was paid to avoid amplification of sequences of other homologous *GSTMs* because exon 8 of *GSTM1* is 99% identical to that of *GSTM2*.[13] We confirmed that PCR fragments were not amplified from samples with *GSTM1*0/*0* genotypes to evaluate primer specificities. The entire *GSTM1* gene except for the region through exon 8 to the 3′-flanking region was amplified in the 1st round of PCR from 25 ng of genomic DNA utilizing 1.25 units of Ex-Taq with 0.2 μM of primers listed in **Table 2**. Next, three regions (from 5′-flanking to exon 3, from exon 4 to 5, and from exon 6 to 7), were separately amplified in the 2nd round PCR from the 1st round PCR product by Ex-Taq (0.625 units) with 0.2 μM primers listed in **Table 2**. The region from exon 8 to the 3′-flanking was separately amplified from 25 ng of genomic DNA using 0.625 units of Ex-Taq with 0.2 μM primers (listed in **Table 2**). All PCR conditions were the same as those described for *GSTT1*. PCR products were then directly sequenced with the primers listed in

Table 1. *GSTT1* primer sequences

	Amplified and sequenced region		Forward primer		Reverse primer		PCR product (bp)
			Sequence (5′ to 3′)	Position[a]	Sequences (5′ to 3′)	Position[a]	
1st round PCR	multiplex	5′-flanking (up to −1366) to exon 1	CACTCCCGCCCCAAATTAGGTT	3776166	ATGATCCCCACCCCTTTATTCG	3774444	1723
		Exon 4 to 3′-flanking region	ATCACAAGGTCAGGAGATTG	3767902	ACTCTTGGCAAACATCAGGG	3766589	1314
		Exon 2	ACATAATCTCTTCTGCAAACTG	3773267	TGTCTCAAGGATACTCTCACCA	3772011	1257
		Exon 3	GCAAATTGTCAGAAAGGTTAAAGA	3770734	CCCACCTCCTGATTAGCTTAGAAG	3768725	2010
2nd round PCR		5′-flanking (up to −801) to exon 1	TTTCAGTGGGATTCGTTTTAGA	3775601	CCCCGTGGTCTATTCCGTGA	3774478	1124
		Exon 4 to 3′-flanking region	CATCACTAATCATTAGGGAA	3767648	CTGGGAAGGGGGTTGTCTTT	3766628	1021
Sequencing		5′-flanking (up to −801)	TTTCAGTGGGATTCGTTTTAGA	3775601	GGCTCGCTCATTTCACTTAG	3775090	
		Exon 1	GGTGGGAAATTCTGACACAC	3775162	CCCCGTGGTCTATTCCGTGA	3774478	
		Exon 2[b]	AAGGGACAAGGTAGTCAGTC	3772758	AACTGGAATAGCAGGAAGGC	3772099	
		Exon 3[b]	AAAAAAAGCGACTATGTATGAAAT	3770153	AGATAAAATGGATGAACAGATGGT	3769662	
		Exon 4	CATCACTAATCATTAGGGAA	3767648	CAGACTGGGGATGGATGGTTGT	3767204	
		Exon 5 to 3′-flanking region	CATCCCCAGTCTGTACCCTTTTCC	3767216	CTGGGAAGGGGGTTGTCTTT	3766628	

[a]The nucleotide position of the 5′ end of each primer on NT_011520.11.
[b]For exons 2 and 3, the 1st round PCR product was directly sequenced.

Table 2. *GSTM1* primer sequences

	Amplified and sequenced region	Forward primer		Reverse primer		PCR product (bp)
		Sequence (5′ to 3′)	Position[a]	Sequences (5′ to 3′)	Position[a]	
1st round PCR	5′-flanking (up to −1309) to exon 7	CCACAAACAAGTTTATTGGGCG	6136872	GTACTAGACATCAATGTCACCGTT	6141347	4476
	Exon 8 to 3′-flanking region	ACAGTGAGATTTTGCTCAGGTATT	6142766	CTCAATTCTAGAAAAGAGCGAG	6145058	2293
2nd round PCR	5′-flanking (up to −650) to exon 3	GACCACATTTCCTTTACTCTGG	6137531	TAAGAATACTGTCACATGAACG	6139231	1701
	Exon 4 to 5	TCTGTGTCCACCTGCATTCGTTCA	6139192	CTGAACACAAACTTTACCATAC	6139883	692
	Exon 6 to 7	CTAATAAATGCTGATGTATCCAAT	6140410	CCTACTATTGCCAGCTCCATCTAT	6141315	906
Sequencing	5′-flanking (up to −650)	GTCCTTCCTATACCACTGACAC	6137567	AACCGAGCAGGGCTCAGAGTAT	6138145	
	Exon 1 to 2	CCCTGACTTCGCTCCCGGAAC	6137956	GGACACCCGTCCCAATTAGACA	6138764	
	Exon 3	TCTGCCCACTCACGCTAAGTTG	6138577	TAAGAATACTGTCACATGAACG	6139231	
	Exon 4 to 5	TCTGTGTCCACCTGCATTCGTTCA	6139192	CTGAACACAAACTTTACCATAC	6139883	
	Exon 6 to 7	CTAATAAATGCTGATGTATCCAAT	6140410	CCTACTATTGCCAGCTCCATCTAT	6141315	
	Exon 8[b]	GAACTTCTGTTTCCCACATGAG	6143164	GAGTAAAGATGGGAATAAACAG	6143735	
	3′-untranslated and flanking region[b]	TCGTTCCTTTCTCCTGTTTATT	6143701	CCTTGGGGTCCTATTCAATGAG	6144362	

[a]The nucleotide position of the 5′ end of each primer on NT_019273.18.
[b]For the region from exon 8 to 3′-flanking, the 1st round PCR product was directly sequenced.

"sequencing" of **Table 2** as described above for *GSTT1*. All novel SNPs were confirmed by repeated sequencing of PCR products that were newly generated by amplification of genomic DNA. The genomic and cDNA sequences of *GSTM1* obtained from GenBank (NT_019273.18 and NM_000561.2, respectively) were used as reference sequences.

Linkage Disequilibrium (LD) and haplotype analyses: Hardy-Weinberg equilibrium and LD analyses were performed by SNPAlyze ver 7.0 (Dynacom Co., Yokohama, Japan). Pairwise LD ($|D'|$ and r^2 values) between two variations was calculated using 102 subjects bearing one or two *GSTT1* genes and 101 subjects bearing one or two *GSTM1* genes. Some haplotypes were unambiguous from subjects with heterozygous **0* alleles. Diplotype configurations were inferred based on estimated haplotype frequencies using Expectation-Maximization algorithms by SNPAlyze software, which can handle multiallelic variations. Haplotypes containing SNPs without any amino acid change were designated as **1*, and nonsynonymous SNP-bearing haplotypes were numerically numbered. Subtypes were named in their frequency order by use of alphabetical small letters.

Results

Determination of deletion polymorphisms in *GSTM1* and *GSTT1*: Both conventional PCR[10] and TaqMan real-time PCR[12] were used to identify deletion of *GSTT1*. By conventional PCR, 92 out of 194 subjects (frequency = 0.474) were assigned as *GSTT1*0/*0*. For all 92 samples with *GSTT1*0/*0*, no significant fluorescence derived from *GSTT1* amplification was detected by TaqMan real-time PCR (mean cycle threshold, Ct, 37.6). Eighty-two (frequency = 0.423) and 20 (frequency = 0.103) subjects were identified as heterozygous (**0/+*) and homozygous (*+/+*) for intact *GSTT1* by conventional PCR, respectively. In the TaqMan real-time PCR, the mean ± SD of relative amounts of *GSTT1* was 1.0 ± 0.111, and 0.448 ± 0.058 for homozygous and heterozygous *GSTT1* carriers, respectively (the mean value for the 20 homozygotes was set as 1). Since the maximum relative amount of *GSTT1* was 1.214, no gene duplication could be inferred for *GSTT1*. The assigned genotypes were consistent between both methods, and their frequencies (**Table 3a**) were in Hardy-Weinberg equilibrium ($p = 0.785$ by Pearson's chi-square test).

As for *GSTM1*, conventional PCR[9] indicated that 93 out of 194 subjects had a homozygous deletion of *GSTM1* (**0/*0*), and that the remaining 101 subjects were either heterozygotes (**0/+*) or homozygotes (*+/+*) for intact *GSTM1*. By real-time PCR, Ct values of 93 samples with the null genotypes were greater than 36.5, which exceeded the sensitivity limits (Ct = 35) of the real-time PCR detection system, indicating that both methods gave consistent results for *GSTM1*0/*0*. As for the 101 subjects with intact *GSTM1* genes (either **0/+* or *+/+*), the distribution of relative amounts of *GSTM1* was clustered into two groups with 1.0 ± 0.083 (16 homozygotes), and 0.51 ± 0.048 (85 heterozygotes) when the mean value of the 16 homozygotes was set as 1. No individuals showed relative amounts more than 1.216, suggesting that the duplication in *GSTM1*[9] was not present in our population. Thus, the frequencies of *GSTM1*0/*0*, **0/+*, and *+/+*, were 0.479, 0.438, and 0.082, respectively (**Table 3a**), and in Hardy-Weinberg equilibrium ($p = 0.576$ by the Pearson's chi-square test).

Table 3b summarizes the results of the distribution of *GSTM1* and *GSTT1* deletions in our Japanese population.

About one-fourth (45 of 194 subjects) were null for both *GSTM1* and *GSTT1* genes.

Variations found in the intact *GSTT1* gene and their LD profiles: Six variations including three novel ones were found by sequencing the 5′-flanking regions, all 5 exons and their flanking regions in the 102 Japanese subjects with **0/+* and *+/+* genotypes (**Table 4**). All detected variations were in Hardy-Weinberg equilibrium ($p \geq 0.44$ by the χ^2 test or Fisher's exact test) when assuming the presence of three alleles (wild, variant and **0* alleles) at each site. One novel nonsynonymous variation, 226C>A (Arg76Ser), was heterozygous in one subject with two intact *GSTT1* genes, and its allele frequency was 0.003 (1/388). The remaining two novel variations in the intronic regions (IVS1+71A>G and IVS2−8A>C) were also rare (allele frequency = 0.003 for both).

Three known variations (IVS1+166A>G, IVS3−36C>T and 824T>C) were found at a relatively high frequency (0.106) and were perfectly linked ($r^2 = 1.0$) with each other.

Table 3. Frequencies of *GSTT1* and *GSTM1* deletions

(a)

	Genotype	N	Frequency (%)	Allele	N	Frequency (%)
GSTT1	**0/*0*	92	0.474	**0*	266	0.686
	**0/+*	82	0.423			
	+/+	20	0.103	*+*	122	0.314
GSTM1	**0/*0*	93	0.479	**0*	271	0.698
	**0/+*	85	0.438			
	+/+	16	0.082	*+*	117	0.302

(b)

Genotype combination		N	Frequency (%)
GSTT1	*GSTM1*		
**0/*0*	**0/*0*	45	0.232
	**0/+*	42	0.216
	+/+	5	0.026
**0/+*	**0/*0*	39	0.201
	**0/+*	34	0.175
	+/+	9	0.046
+/+	**0/*0*	9	0.046
	**0/+*	9	0.046
	+/+	2	0.010

**0*, deletion; *+*, intact gene

Variations found in the intact *GSTM1* gene and their LD profile: We found 23 variations, including seven novel ones, in 194 Japanese cancer patients (**Table 5**). Ten variations were located in the 5′-flanking region, 2 in the coding exons, 9 in the introns, and 2 in the 3′-flanking region. All detected variations were in Hardy-Weinberg equilibrium ($p > 0.37$ by the χ^2 test or Fisher's exact test) except for 1107+41C>T in the 3′-flanking region ($p = 0.003$ by the Fisher's exact test). Deviation from Hardy-Weinberg equilibrium for this variation was due to 2 more homozygotes than expected among 16 *GSTM1* +/+ subjects.

Seven novel variations, −416G>T and −165A>G in the 5′-flanking region, IVS1+97C>T, IVS1−79G>A, IVS1−78T>A, and IVS2+202G>A in the introns and 1107+128G>A in the 3′-flanking region, were found in single subjects (allele frequencies = 0.003). No novel nonsynonymous SNPs were detected.

Sixteen other variations were already reported or publicized in the dbSNP and/or JSNP databases. They were detected in more than 10 chromosomes (allele frequencies ≥0.026) in our population except for −423C>G and IVS2+118T>C (allele frequency = 0.003).

The pairwise |D′| values between 14 common variations (N≥10) in *GSTM1* were higher than 0.95 except for the combinations between −480A>G and other variations, which showed lower |D′| values ($0.27 < |D'| < 1.0$). As for the r^2 values, strong LDs ($r^2 > 0.87$) were observed among 10 variations,

Table 4. Summary of *GSTT1* SNPs detected in a Japanese population

SNP ID			Location	Position		Nucleotide change and flanking sequences (5′ to 3′)	Amino acid change	Allele frequency (N=388)
This study	dbSNP (NCBI)	JSNP		NT_011520.11	From the translational initiation site or from the end of nearest exon			
MPJ6_GTT1001[a]			intron1	3774618	IVS1+71A>G	catagcttagggA/Gacttctcccagc		0.003
MPJ6_GTT1002	rs140313	ssj0002194	intron1	3774523	IVS1+166A>G	gatccaagagtcA/Ggggctccccaaa		0.106
MPJ6_GTT1003[a]			intron2	3770088	IVS2-8A>C	catgacccccacA/Ccccacagtgtgg		0.003
MPJ6_GTT1004[a]			Exon3	3770055	226C>A	ctctacctgacgC/Agcaaatataagg	Arg76Ser	0.003
MPJ6_GTT1005	rs140308		intron3	3767603	IVS3-36C>T	ctaactccctacC/Tccagtaactccc		0.106
MPJ6_GTT1006	rs4630	ssj0002197	3′-UTR	3766891	824(*101[b])T>C	ggaatggcttgcT/Ctaagacttgccc		0.106

[a]Novel variations detected in this study.
[b]The nucleotide that follows the translation termination codon TGA is numbered and starts as *1.

Table 5. Summary of *GSTM1* SNPs detected in a Japanese population

SNP ID			Location	Position		Nucleotide change and flanking sequences (5′ to 3′)	Amino acid change	Reported alleles	Allele frequency (N = 388)
This study	dbSNP (NCBI)	JSNP		NT_019273.18	From the translational initiation site or from the end of nearest exon				
MPJ6_GTM1001	rs412543	ssj0002146	5′-flanking	6137629	−552C>G	agactaagccct**C/G**ggagtagctttc			0.044
MPJ6_GTM1002	rs3815029	ssj0002147	5′-flanking	6137641	−540C>G	gggagtagctttt**C/G**gatcagaggaa			0.026
MPJ6_GTM1003	rs412302	ssj0002148	5′-flanking	6137701	−480A>G	tcccaggttggg**A/G**ccaccacttttt			0.064
MPJ6_GTM1004	rs3815026		5′-flanking	6137758	−423C>G	cccttgggaact**C/G**gcagcggagag			0.003
MPJ6_GTM1005[a]			5′-flanking	6137765	−416G>T	gaactcggcagc**G/T**gagagaaggctg			0.003
MPJ6_GTM1006	rs4147561	ssj0002149	5′-flanking	6137783	−398C>T	aaggctgaggga**C/T**accgcgggcagg			0.077
MPJ6_GTM1007	rs4147562	ssj0002150	5′-flanking	6137784	−397A>T	aggctgagggac**A/T**ccgcgggcaggg			0.077
MPJ6_GTM1008	rs4147563	ssj0002151	5′-flanking	6137788	−393T>C	tgagggacaccg**T/C**gggcagggagga			0.080
MPJ6_GTM1009	rs28549287	ssj0002152	5′-flanking	6137823	−358G>A	gagctttgctcc**G/A**ttaggatctggc			0.075
MPJ6_GTM1010[a]			5′-flanking	6138016	−165A>G	cttactgagtgc**A/G**gccccaggcgcc			0.003
MPJ6_GTM1011[a]			intron1	6138313	IVS1+97C>T	tcctcttcaggg**C/T**tgcccgcctcag			0.003
MPJ6_GTM1012[a]			intron1	6138398	IVS1−79G>A	ggtacgtgcagt**G/A**taaactgggggc			0.003
MPJ6_GTM1013[a]			intron1	6138399	IVS1−78T>A	gtacgtgcagtg**T/A**aaactgggggct			0.003
MPJ6_GTM1014	rs4147564	ssj0002153	intron2	6138670	IVS2+118T>C	ctgcaggctgtc**T/C**cttccctgagcc			0.003
MPJ6_GTM1015[a]			intron2	6138754	IVS2+202G>A	ctgtctaattgg**G/A**acgggtgtccct			0.003
MPJ6_GTM1016	rs737497	ssj0002154	intron3	6139277	IVS3−78C>T	cccggtctcctc**C/T**ctgctcttgctt			0.077
MPJ6_GTM1017	rs4147565	ssj0002155	intron4	6139462	IVS4+26A>G	gctgcaatgtgt**A/G**gggggaaggtgg			0.080
MPJ6_GTM1018	rs4147566	ssj0002156	intron5	6139772	IVS5+140C>T	cagttattctca**C/T**gactccaatgtc			0.077
MPJ6_GTM1019	rs1065411	ssj0002159	Exon7	6140823	519C>G	atttgagcccaa**C/G**tgcttggacgcc	Asn173Lys	*B	0.077
MPJ6_GTM1020	rs1056806	ssj0002160	Exon7	6140832	528C>T	caagtgcttgga**C/T**gccttcccaaat	Asp176Asp		0.077
MPJ6_GTM1021	rs4147569	ssj0002161	intron7	6143292	IVS7−221G>A	tgtagaatcttc**G/A**taagtgttagct			0.080
MPJ6_GTM1022	rs4147570	ssj0002162	3′-flanking	6144093	1107(*450)+41C>T[b]	ctggccatctac**C/T**cagactgtctgt			0.026
MPJ6_GTM1023[a]			3′-flanking	6144180	1107(*450)+128G>A[b]	ggattctgctgg**G/A**catagtaaggcg			0.003

[a]Novel variations detected in this study.
[b]The position of the 3′ end of exon 8 (1107 or *450)+the position in the 3′-flanking region. (*450 indicates the position from the termination codon TAG.)

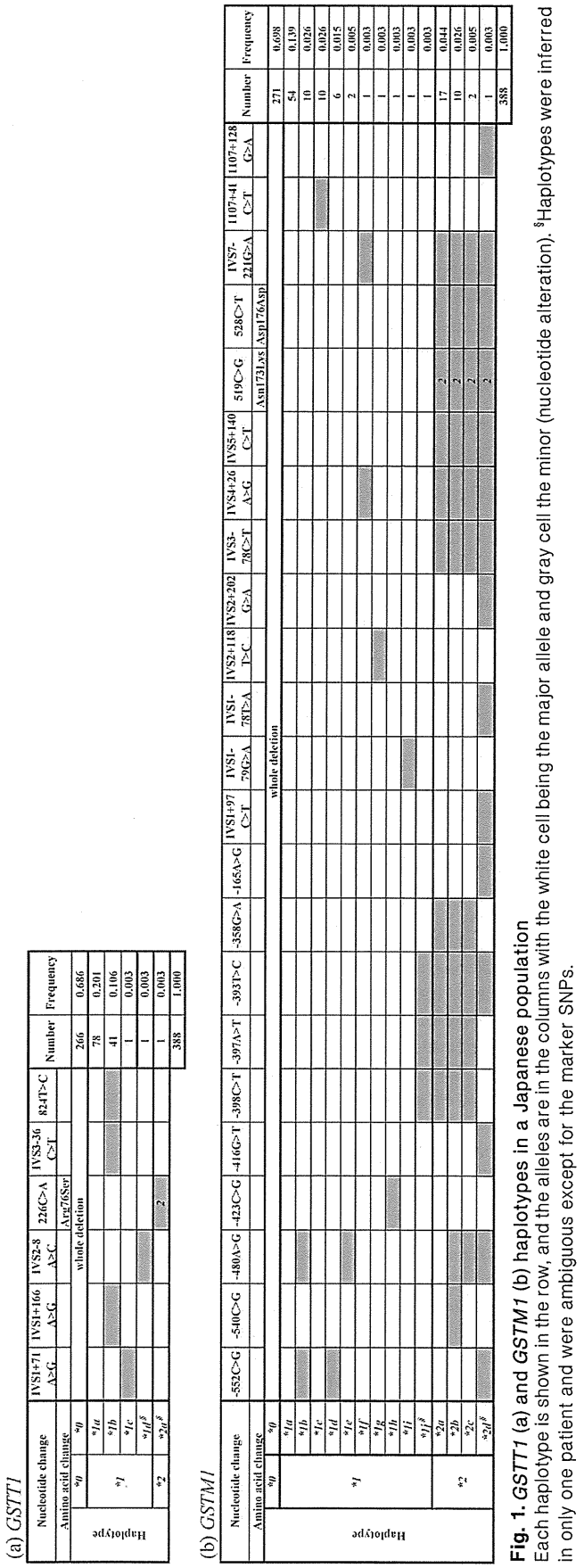

Fig. 1. *GSTT1* (a) and *GSTM1* (b) haplotypes in a Japanese population
Each haplotype is shown in the row, and the alleles are in the columns with the white cell being the major allele and gray cell the minor (nucleotide alteration). §Haplotypes were inferred in only one patient and were ambiguous except for the marker SNPs.

−398C>T, −397A>T, −393T>C, −358G>A, IVS3−78C>T, IVS4+26A>G, IVS5+140C>T, 519C>G (Asn173Lys), 528C>T (Asp176Asp), and IVS7−221G>A. Of these variations, two (−398C>T and −397A>T) and four (IVS3−78C>T, IVS5+140C>T, 519C>G, and 528C>T) pairs of SNPs were in perfect LD ($r^2 = 1.0$).

Haplotype estimation and selection of haplotype-tagging SNPs (htSNPs): Based on results of the LD profiles, haplotypes of *GSTT1* and *GSTM1* were analyzed as one LD block that spans at least 7.7 kb and 6.5 kb, respectively. Using the six variations and null alleles in *GSTT1*, three common haplotypes (*GSTT1*0*, **1a* and **1b*) and three rare haplotypes (**1c*, **1d* and **2a*) were identified or inferred (**Fig. 1a**). Frequencies of the common haplotypes, **0*, **1a*, and **1b*, were 0.686, 0.201, and 0.106, respectively. Thus, the htSNPs are either one of IVS1+166A>G, IVS3−36C>T, and 824T>C for **1b* and 226C>A for **2*.

For the *GSTM1* gene, three groups of haplotypes (*GSTM1*0*, **1* and **2*), each containing 1, 10 and 4 subtypes, were identified or inferred using the 23 variations and the null allele (**Fig. 1b**). The **2* group (**2a* to **2d*) was defined as the haplotypes harboring the known nonsynonymous SNP, 519C>G (Asn173Lys), which was previously assigned **B*.[8] The most dominant haplotype was **0* (0.698 frequency), followed by **1a* (0.139), **2a* (0.044), **1b* (0.026), **1c* (0.026), and **2b* (0.026). These six haplotypes accounted for 95% of all haplotypes. The htSNPs that were able to resolve the 5 common haplotypes of the intact genes were −552C>G (**1b* and **1d*), −540C>G (**2b*), −480A>G (**1b* and **2b*), 519C>G (Asn173Lys) (**2*), and 1107+41C>T (**1c*).

Discussion

The present study provides the first comprehensive data on genetic variations of *GSTT1* and *GSTM1* in Japanese, the genes encoding the phase II metabolic enzymes important for cellular defense systems. Moreover, SNPs in intact genes were identified by resequencing, and haplotype structures and tagging SNPs were shown.

It is well recognized that **0* alleles in *GSTT1* and *GSTM1* distribute with different frequencies in several ethnicities. We have shown that 47.4% and 47.9% of our Japanese population homozygously lack *GSTT1* (*GSTT1*0/*0*) and *GSTM1* (*GSTM1*0/*0*), respectively. The *GSTT1*0/*0* frequency is comparable to that reported previously in Japanese (54.0%)[14] and east Asians such as Koreans (46–62%)[7,15] and Chinese (49–58%),[16,17] but was higher than Malay (38%),[17] Indians (16%),[17] Caucasians (15–24%),[7,18] African Americans (22–24%),[7,18] Mexican Americans (10%),[7] and Scandinavians (15%).[7] On the other hand, no marked differences are found in the frequencies of *GSTM1*0/*0* between Caucasians (42–60%)[7,18] and East Asians including Japanese, Koreans

and Chinese (44–63%),[7,14–16] although these frequencies were higher than that of Africans (16–36%).[7,18] The subjects bearing neither *GSTT1* nor *GSTM1* were observed at 23.2%, the frequency of which is similar to Koreans (29.1%)[15] and Shanghai Chinese (24%),[16] but higher than Caucasians (7.5–10.4%)[7,18] and Africans (3.9%).[18]

A number of association studies of the *GSTM1* and *GSTT1* genotypes with cancer susceptibility and cancer therapy outcome have been reported; however, the results are sometimes conflicting.[5–7] In our 194 patients with mainly non-small cell lung cancers, the frequency of *GSTT1*0/*0* and *GSTM1*0/*0* was similar to those in healthy Japanese. This result is in good agreement with a body of literature where the effects of *GSTT1* and *GSTM1* null genotypes on lung cancer development were not clear unless other genetic traits affecting carcinogen metabolism such as *CYP1A1*2A* and *GSTP1*B* (Ile105Val) were combined.[7]

One novel *GSTT1* nonsynonymous variation (226C>A, Arg76Ser) was found in one subject. Arg76 is located in the α3 helix of N-terminal domain I, which forms glutathione binding sites.[19,20] In the crystal structure of human GSTT1-1, this residue closely (2.7 Å) contacts Tyr85 of another subunit (Protein Data Bank, 2C3T).[21] Arg76 is conserved among human, bovine and chicken, whereas this residue is a histidine in mouse and rat. Interestingly, rat and mouse GSTT2 have Ser at position 76.

Of the six SNPs detected in *GSTT1*, three were perfectly linked, resulting in a simple haplotype structure. One of the linked SNPs, 824T>C, was analyzed for various ethnicities in the SNP500Cancer Database (http://snp500cancer.nci.nih.gov/). Its frequency in Japanese (0.106) was comparable to that in Caucasians (0.121), but lower than that in Africans and African-Americans (0.70).

In the *GSTM1* 5′-flanking region (up to −650), eight known SNPs in the NCBI dbSNP database were also detected in this study. This was in contrast to *GSTT1*, in which no SNPs were detected in the 5′-flanking region (up to −801 bp). Murine GSTM1 is transcriptionally upregulated by the Myb proto-oncogene protein through the Myb-binding site (−58 to −63) in the *GSTM1* promoter,[22] whereas no studies on the mechanisms of transcriptional regulation have been performed with human GSTM1. The four common SNPs, −398C>T, −397A>T, −393T>C, and −358G>A (0.075–0.080 in frequencies), were almost perfectly linked with the known SNP, 519C>G (Asn173Lys, *GSTM1*B*) in Japanese. The GSTM1a-1a isozyme (Asn173) and GSTM1b-1b isozyme (Lys173) were reported to have similar catalytic activities *in vitro*.[8] Nevertheless the association of the *GSTM1*A* alleles has been shown with a reduced risk for bladder cancer.[23] Therefore, the functional significance of promoter SNPs on *GSTM1* expression should be further elucidated.

In conclusion, deletions of *GSTT1* and *GSTM1* in Japanese were analyzed by conventional PCR and TaqMan real-time PCR. About one-fourth (0.232 in frequency) of subjects had double *GSTM1* and *GSTT1* null genotypes. In the intact *GSTT1* and *GSTM1* genes, six and 23 SNPs were identified, respectively, and three (*GSTT1*0*, **1a*, **1b*) and six (*GSTM1*0*, **1a*, **2a*, **1b*, **1c* and **2b*) common haplotypes were inferred. Only one rare nonsynonymous SNP (226C>A, Arg76Ser) was found in *GSTT1*, suggesting that this gene is highly conserved. These findings would be useful for pharmacogenetic studies that investigate the relationship between the efficacy of anticancer drugs and *GST* haplotypes.

Acknowledgments: We thank Ms. Chie Sudo for her secretarial assistance.

References

1) Chasseaud, L. F.: The role of glutathione and glutathione *S*-transferases in the metabolism of chemical carcinogens and other electrophilic agents. *Adv. Cancer Res.*, **29**: 175–274 (1979).
2) Hayes, J. D. and McLellan, L. I.: Glutathione and glutathione-dependent enzymes represent a co-ordinately regulated defence against oxidative stress. *Free Radic. Res.*, **31**: 273–300 (1999).
3) Adler, V., Yin, Z., Fuchs, S. Y., Benezra, M., Rosario, L., Tew, K. D., Pincus, M. R., Sardana, M., Henderson, C. J., Wolf, C. R., Davis, R. J. and Ronai, Z.: Regulation of JNK signaling by GSTp. *Embo J.*, **18**: 1321–1334 (1999).
4) Listowsky, I., Abramovitz, M., Homma, H. and Niitsu, Y.: Intracellular binding and transport of hormones and xenobiotics by glutathione-*S*-transferases. *Drug Metab. Rev.*, **19**: 305–318 (1988).
5) Hayes, J. D. and Strange, R. C.: Glutathione S-transferase polymorphisms and their biological consequences. *Pharmacology*, **61**: 154–166 (2000).
6) McIlwain, C. C., Townsend, D. M. and Tew, K. D.: Glutathione *S*-transferase polymorphisms: cancer incidence and therapy. *Oncogene*, **25**: 1639–1648 (2006).
7) Bolt, H. M. and Thier, R.: Relevance of the deletion polymorphisms of the glutathione *S*-transferases GSTT1 and GSTM1 in pharmacology and toxicology. *Curr. Drug. Metab.*, **7**: 613–628 (2006).
8) Widersten, M., Pearson, W. R., Engstrom, A. and Mannervik, B.: Heterologous expression of the allelic variant mu-class glutathione transferases mu and psi. *Biochem. J.*, **276 (Pt 2)**: 519–524 (1991).
9) McLellan, R. A., Oscarson, M., Alexandrie, A. K., Seidegard, J., Evans, D. A., Rannug, A. and Ingelman-Sundberg, M.: Characterization of a human glutathione *S*-transferase mu cluster containing a duplicated GSTM1 gene that causes ultrarapid enzyme activity. *Mol. Pharmacol.*, **52**: 958–965 (1997).
10) Sprenger, R., Schlagenhaufer, R., Kerb, R., Bruhn, C., Brockmoller, J., Roots, I. and Brinkmann, U.: Characterization of the glutathione *S*-transferase GSTT1 deletion: discrimination of all genotypes by polymerase chain reaction indicates a trimodular genotype-phenotype correlation. *Pharmacogenetics*, **10**: 557–

565 (2000).

11) Seidegard, J., Vorachek, W. R., Pero, R. W. and Pearson, W. R.: Hereditary differences in the expression of the human glutathione transferase active on trans-stilbene oxide are due to a gene deletion. *Proc. Natl. Acad. Sci. U S A*, **85**: 7293–7297 (1988).
12) Covault, J., Abreu, C., Kranzler, H. and Oncken, C.: Quantitative real-time PCR for gene dosage determinations in microdeletion genotypes. *Biotechniques*, **35**: 594–596, 598 (2003).
13) Vorachek, W. R., Pearson, W. R. and Rule, G. S.: Cloning, expression, and characterization of a class-mu glutathione transferase from human muscle, the product of the GST4 locus. *Proc. Natl. Acad. Sci. U S A*, **88**: 4443–4447 (1991).
14) Naoe, T., Takeyama, K., Yokozawa, T., Kiyoi, H., Seto, M., Uike, N., Ino, T., Utsunomiya, A., Maruta, A., Jin-nai, I., Kamada, N., Kubota, Y., Nakamura, H., Shimazaki, C., Horiike, S., Kodera, Y., Saito, H., Ueda, R., Wiemels, J. and Ohno, R.: Analysis of genetic polymorphism in NQO1, GST-M1, GST-T1, and CYP3A4 in 469 Japanese patients with therapy-related leukemia/ myelodysplastic syndrome and de novo acute myeloid leukemia. *Clin. Cancer Res.*, **6**: 4091–4095 (2000).
15) Cho, H. J., Lee, S. Y., Ki, C. S. and Kim, J. W.: GSTM1, GSTT1 and GSTP1 polymorphisms in the Korean population. *J. Korean Med. Sci.*, **20**: 1089–1092 (2005).
16) Shen, J., Lin, G., Yuan, W., Tan, J., Bolt, H. M. and Thier, R.: Glutathione transferase T1 and M1 genotype polymorphism in the normal population of Shanghai. *Arch Toxicol*, **72**: 456–458 (1998).
17) Lee, E. J., Wong, J. Y., Yeoh, P. N. and Gong, N. H.: Glutathione *S* transferase-theta (GSTT1) genetic polymorphism among Chinese, Malays and Indians in Singapore. *Pharmacogenetics*, **5**: 332–334 (1995).
18) Chen, C. L., Liu, Q. and Relling, M. V.: Simultaneous characterization of glutathione *S*-transferase M1 and T1 polymorphisms by polymerase chain reaction in American whites and blacks. *Pharmacogenetics*, **6**: 187–191 (1996).
19) Armstrong, R. N.: Structure, catalytic mechanism, and evolution of the glutathione transferases. *Chem. Res. Toxicol.*, **10**: 2–18 (1997).
20) Frova, C.: Glutathione transferases in the genomics era: new insights and perspectives. *Biomol. Eng.*, **23**: 149–169 (2006).
21) Tars, K., Larsson, A. K., Shokeer, A., Olin, B., Mannervik, B. and Kleywegt, G. J.: Structural basis of the suppressed catalytic activity of wild-type human glutathione transferase T1–1 compared to its W234R mutant. *J. Mol. Biol.*, **355**: 96–105 (2006).
22) Bartley, P. A., Keough, R. A., Lutwyche, J. K. and Gonda, T. J.: Regulation of the gene encoding glutathione *S*-transferase M1 (GSTM1) by the Myb oncoprotein. *Oncogene*, **22**: 7570–7575 (2003).
23) Brockmoller, J., Kerb, R., Drakoulis, N., Staffeldt, B. and Roots, I.: Glutathione *S*-transferase M1 and its variants A and B as host factors of bladder cancer susceptibility: a case-control study. *Cancer Res*, **54**: 4103–4111 (1994).